Research Paper

GEOSPHERE

GEOSPHERE, v. 17

https://doi.org/10.1130/GES02289.1

11 figures; 3 tables; 1 supplemental file

CORRESPONDENCE: GuiceG@si.edu

CITATION: Guice, G.L., Ackerson, M.R., Holder, R.M., George, F.R., Browning-Hanson, J.F., Burgess, J.L., Foustoukos, D.I., Becker, N.A., Nelson, W.R., and Viete, D.R., 2021, Suprasubduction zone ophiolite fragments in the central Appalachian orogen: Evidence for mantle and Moho in the Baltimore Mafic Complex (Maryland, USA): Geosphere, v. 17, https://doi.org/10.1130/GES02289.1.

Science Editor: Andrea Hampel
Associate Editor: Alan Whittington

Received 22 May 2020
Revision received 4 September 2020
Accepted 22 December 2020

Suprasubduction zone ophiolite fragments in the central Appalachian orogen: Evidence for mantle and Moho in the Baltimore Mafic Complex (Maryland, USA)

George L. Guice[1], Michael R. Ackerson[1], Robert M. Holder[2,3], Freya R. George[2], Joseph F. Browning-Hanson[2], Jerry L. Burgess[2], Dionysis I. Foustoukos[4], Naomi A. Becker[2], Wendy R. Nelson[5], and Daniel R. Viete[2]

[1]Department of Mineral Sciences, National Museum of Natural History, Smithsonian Institution, 10th Street and Constitution Avenue NW, Washington, D.C. 20560, USA
[2]Department of Earth and Planetary Sciences, Johns Hopkins University, 3400 N Charles Street, Baltimore, Maryland 21218, USA
[3]Department of Earth and Environmental Sciences, University of Michigan, 1100 N University Avenue, Ann Arbor, Michigan 48109, USA
[4]Earth and Planets Lab, Carnegie Institution of Washington, 5251 Broad Branch Road NW, Washington, D.C. 20015, USA
[5]Department of Physics, Astronomy, and Geoscience, Towson University, 8000 York Road, Towson, Maryland 21252, USA

ABSTRACT

Suprasubduction zone (SSZ) ophiolites of the northern Appalachians (eastern North America) have provided key constraints on the fundamental tectonic processes responsible for the evolution of the Appalachian orogen. The central and southern Appalachians, which extend from southern New York to Alabama (USA), also contain numerous ultramafic-mafic bodies that have been interpreted as ophiolite fragments; however, this interpretation is a matter of debate, with the origin(s) of such occurrences also attributed to layered intrusions. These disparate proposed origins, alongside the range of possible magmatic affinities, have varied potential implications for the magmatic and tectonic evolution of the central and southern Appalachian orogen and its relationship with the northern Appalachian orogen. We present the results of field observations, petrography, bulk-rock geochemistry, and spinel mineral chemistry for ultramafic portions of the Baltimore Mafic Complex, which refers to a series of ultramafic-mafic bodies that are discontinuously exposed in Maryland and southern Pennsylvania (USA). Our data indicate that the Baltimore Mafic Complex comprises SSZ ophiolite fragments. The Soldiers Delight Ultramafite displays geochemical characteristics—including highly depleted bulk-rock trace element patterns and high Cr# of spinel—characteristic of subduction-related mantle peridotites and serpentinites. The Hollofield Ultramafite likely represents the "layered ultramafics" that form the Moho. Interpretation of the Baltimore Mafic Complex as an Iapetus Ocean–derived SSZ ophiolite in the central Appalachian orogen raises the possibility that a broadly coeval suite of ophiolites is preserved along thousands of kilometers of orogenic strike.

George Guice https://orcid.org/0000-0003-0599-0907

INTRODUCTION

The Appalachian orogen in eastern North America—a product of the protracted closure of the Iapetus and Rheic Oceans during the Paleozoic Era—contains numerous discrete ultramafic-mafic bodies along its 3000 km length (Misra and Keller, 1978). Such bodies are generally a minor component of orogenic belts such as the Appalachians, but determining their origin(s) can place important constraints on broader magmatic and tectonic histories (e.g., Lissenberg et al., 2005). End-member interpretations of these bodies are that they represent ophiolite fragments (Crowley, 1976) or layered intrusions (Sinha et al., 1997; Kerrigan et al., 2017). These two first-order interpretations require very different tectono-magmatic origins: obduction or emplacement of oceanic lithosphere onto or into continental lithosphere; or the intrusion of mafic magma in a continental setting.

Beyond these basic interpretations, the magmatic affinity of the ultramafic-mafic bodies also has significant implications for the geodynamic processes that formed the Appalachian orogen. For example, in the northernmost Appalachians (Newfoundland and Québec, Canada), the ultramafic-mafic bodies are widely interpreted as near-complete to significantly tectonized suprasubduction zone ophiolites that have been tectonically juxtaposed with the surrounding rocks (Church and Stevens, 1971; Williams, 1977; Huot et al., 2002; Kim et al., 2003; Coish and Gardner, 2004; Kurth-Velz et al., 2004; Lissenberg et al., 2005; Monteiro et al., 2008; Escayola et al., 2011). This interpretation constrains the ultramafic-mafic bodies as representing forearc (or back-arc) oceanic lithosphere that formed due to seafloor spreading in a subduction zone setting (e.g., Whattam and Stern, 2011; Stern et al., 2012).

In the central and southern Appalachians, the petrogenesis and origin(s) of the comparatively small, yet numerous, ultramafic-mafic bodies are poorly understood (Crowley, 1976; Misra and Keller, 1978; Hanan and Sinha, 1989; Sinha et al., 1997; Peterson and Ryan, 2009). Several occurrences are interpreted as the dismembered fragments of ophiolites, including: amphibolites and associated units of the Dadeville Complex, Alabama (Stow et al., 1984); the Hamlett Grove meta-igneous suite, South Carolina (Mittwede, 1989); the Buck Creek ultramafic body and associated ultramafic-mafic bodies within the Ashe and Alligator Back Metamorphic Suites, North Carolina (McElhaney and McSween, 1983; Misra and Conte, 1991; Tenthorey

et al., 1996; Raymond et al., 2003, 2016; Peterson and Ryan, 2009); the Piney Branch Complex, Virginia (Drake and Morgan, 1981); and the Baltimore Mafic Complex (BMC), Maryland–southern Pennsylvania (Crowley, 1976). However, none of the proposed ophiolites in the central and southern Appalachians have been definitively shown to contain residual mantle rocks (Shank and Marquez, 2014).

Mantle rocks, which comprise the lowermost portions of oceanic lithosphere (e.g., Dilek and Furnes, 2011, 2014, and references therein), exhibit characteristically depleted trace element abundances and are therefore the most chemically unique portion of ophiolites (e.g., Paulick et al., 2006; Godard et al., 2008). This geochemical signature results from the preferential concentration of incompatible trace elements in the melt during partial melting, resulting in their extraction from, and subsequent depletion in, the upper mantle (e.g., Godard et al., 2008; Stern et al., 2012). Unequivocal demonstration of the presence of residual mantle rocks in any of these central or southern Appalachian ultramafic-mafic complexes would provide robust evidence in favor of an ophiolite hypothesis. This, coupled with a greater understanding of the magmatic affinity of these bodies, would be a valuable constraint for magmatic and tectonic reconstructions of the Appalachian orogen.

The BMC is the largest ultramafic-mafic body preserved in the central or southern Appalachians (Southwick, 1969; Crowley, 1976; Hanan and Sinha, 1989; Sinha et al., 1997). Its occurrence has been interpreted as representing: fragments of an ophiolite (Crowley, 1976); or a stratiform intrusion (Shank and Marquez, 2014) derived from magmatism associated with either a continental volcanic arc (Sinha et al., 1997) or back-arc basin (Hanan and Sinha, 1989). In this study, we present the results of field observations, petrography, bulk-rock geochemistry, and spinel group mineral chemistry for ultramafic samples from the BMC (Fig. 1). Using the presented data, we evaluate the validity of the previously proposed models for the origin of the BMC (i.e., ophiolite or intrusion), with a focus on establishing whether any of the studied rocks resemble the chemically distinctive residual mantle rocks that have been confidently recognized in ultramafic-mafic complexes of the northern Appalachian orogen. We also consider the magmatic affinity of the BMC and discuss potential implications for the evolution of the Appalachian orogen.

GEOLOGICAL FRAMEWORK

The Appalachian Orogen

The Appalachian orogen is a northeast-southwest–trending belt of Mesoproterozoic to Paleozoic rocks that are exposed over a distance of 3000 km in North America, from Alabama in the south to Newfoundland in the north (Rodgers, 1968; Aleinikoff et al., 2002; Hibbard et al., 2007b; Hatcher, 2010; Horton et al., 2010; Sinha et al., 2012). It is commonly separated into northern, central, and southern segments (see Fig. 1) that reflect distinctions in terms of protolith age, lithology, metamorphism, and deformation (Rodgers, 1970; Hibbard et al., 2007b; Hatcher, 2010; Sinha et al., 2012; Bosbyshell et al., 2016). Along its entire strike, the Appalachian orogen is subdivided into three tectonic realms with distinctive provenance, namely (from west to east; Rodgers, 1970; Rankin, 1975; Adams et al., 1994; Hibbard et al., 1998, 2007b, 2007a; Hatcher, 1987; Murphy et al., 2010):

- The Laurentian realm, comprising rocks deposited either on or immediately adjacent to the Laurentian paleocontinent;
- The Iapetan realm (often referred to as the "Piedmont domain"; Hibbard et al., 2007b), which records the evolution of the Iapetus Ocean, including the development of volcanic arcs, back-arc basins, and accretionary complexes; and
- The Peri-Gondwanan realm, comprising rocks that formed proximal to the Gondwanan paleocontinent prior to its accretion to eastern Laurentia.

The Laurentian realm is remarkably uniform along strike, with rift-drift lithologies and overlying sedimentary rocks showing limited first-order variation from Alabama to Newfoundland (Rodgers, 1968; Thomas, 1977; Lavoie et al., 2003). In contrast, the Iapetan and Peri-Gondwanan realms show considerable variability and have been further subdivided into a series of terranes that record unique ages, lithologies, metamorphic grades, and structural styles (e.g., Williams and Hatcher, 1982; Horton et al., 1989; Faill, 1997; Hatcher, 2004, 2010; Sinha et al., 2012). In the central and southern Appalachians, the Iapetan realm comprises volcano-sedimentary rocks of arc and oceanic affinities, while the Peri-Gondwanan realm records Gondwanan arc magmatism and sedimentation (Hibbard et al., 1998, 2007b). In places, these Neoproterozoic–Paleozoic rocks are overlain by Carboniferous clastic sedimentary rocks, Mesozoic volcano-sedimentary units, and the dominantly Cenozoic sediments of the Atlantic coastal plain (Fig. 1A).

The Baltimore Mafic Complex (BMC)

The BMC of the central Appalachians (located within the Iapetan realm; Fig. 1A) is a series of ultramafic-mafic bodies that are discontinuously exposed in Maryland and southern Pennsylvania. These rocks have been extensively studied over the past 120 years (Leonard, 1901; Bascom, 1902; Hopson, 1964; Higgins et al., 1977; Hanan and Sinha, 1989; Gates, 1992; Sinha et al., 1997; Gates et al., 1999; Burgess et al., 2009; Shank and Marquez, 2014), though southern (Baltimore region, Maryland) portions of the BMC have received scant attention in the past 25 years. The largest of the ultramafic-mafic bodies in the southern BMC is located west of Baltimore and includes the Mount Washington Amphibolite and Hollofield Ultramafite (Fig. 1B; Drake, 1998). Smaller ultramafic-mafic bodies nearby include the Raspeburg Amphibolite, Soldiers Delight Ultramafite, and a small exposure of ultramafic rocks at Bare Hills (Fig. 1B). Near the Maryland-Pennsylvania border (the northern BMC), a large ultramafic-mafic body—known as the State Line Complex—is well exposed either side of the Susquehanna River (Gates, 1992; Burgess et al., 2009; Shank and Marquez, 2014). Notably, the Soldiers Delight and Bare Hills occurrences were mined for chromium—a commodity typically associated with ultramafic rocks of varied origins (see

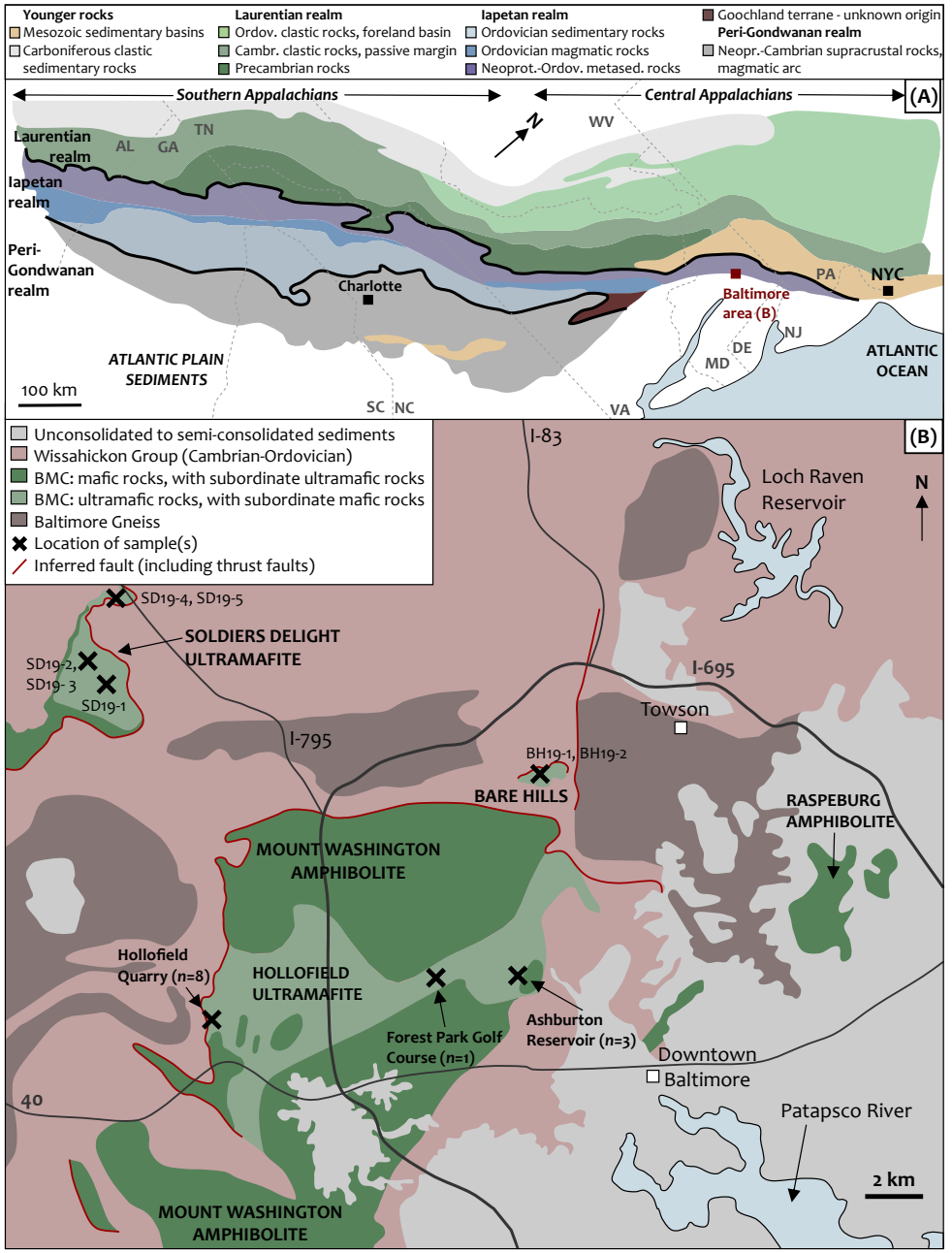

Figure 1. (A) Simplified lithostratigraphic map of the central and southern Appalachian orogen (redrawn after Hibbard, 2006). AL—Alabama; GA—Georgia; DE—Delaware; MD—Maryland; NJ—New Jersey; NC—North Carolina; NYC—New York City; PA—Pennsylvania; SC—South Carolina; TN—Tennessee; VA—Virginia. (B) Simplified geologic map of the Baltimore area, detailing the distribution of samples collected as part of this study (redrawn after Cleaves et al., 1974; Crowley et al., 1975; Crowley, 1976; Reinhardt and Crowley, 1979; Crowley and Reinhardt, 1979). BMC—Baltimore Mafic Complex; I—Interstate Highway.

Cawthorn et al., 2005)—during the 19th and 20th centuries (Johnsson, 2017).

Contacts between the BMC and surrounding rocks—predominantly Mesoproterozoic gneiss and Neoproterozoic–Cambrian volcano-sedimentary rocks of the Wissahickon Group (Fig. 1B; Horton et al., 1989; Faill, 1997; Gates et al., 1999; Aleinikoff et al., 2002)—are poorly exposed but generally tectonic where observed. Ordovician granite locally intrudes the State Line Complex (Crowley, 1976; Hanan and Sinha, 1989; Burgess et al., 2009; Shank and Marquez, 2014). U-Pb zircon geochronology conducted on mafic rocks from the southern BMC yielded a crystallization age of 489 ± 7 Ma (Sinha et al., 1997), which is consistent with multi-mineral Sm-Nd geochronology that returned an isochron age of 490 ± 20 Ma (Shaw and Wasserburg, 1984). The ultramafic components comprise serpentinized dunite and peridotite alongside relict websterite and dunite kernels, with these lithologies considered to form the stratigraphic base of the BMC (Sinha et al., 1997; Shank and Marquez, 2014). The overlying mafic rocks comprise massive and layered gabbronorite, gabbro, amphibolite, and quartz gabbro, alongside minor aplite and diorite (Southwick, 1969; Crowley, 1976; Hanan and Sinha, 1989; Sinha et al., 1997; Burgess et al., 2009). The BMC has experienced considerable metamorphism—dated at 453 ± 11 Ma by Sinha et al. (1997)—and hydrothermal alteration, with a series of northeast-trending dextral transcurrent shear zones occurring within the 5-km-thick section exposed along the Susquehanna River (Burgess et al., 2009). Individual 0.2–1.4-km-wide shear zones are defined by

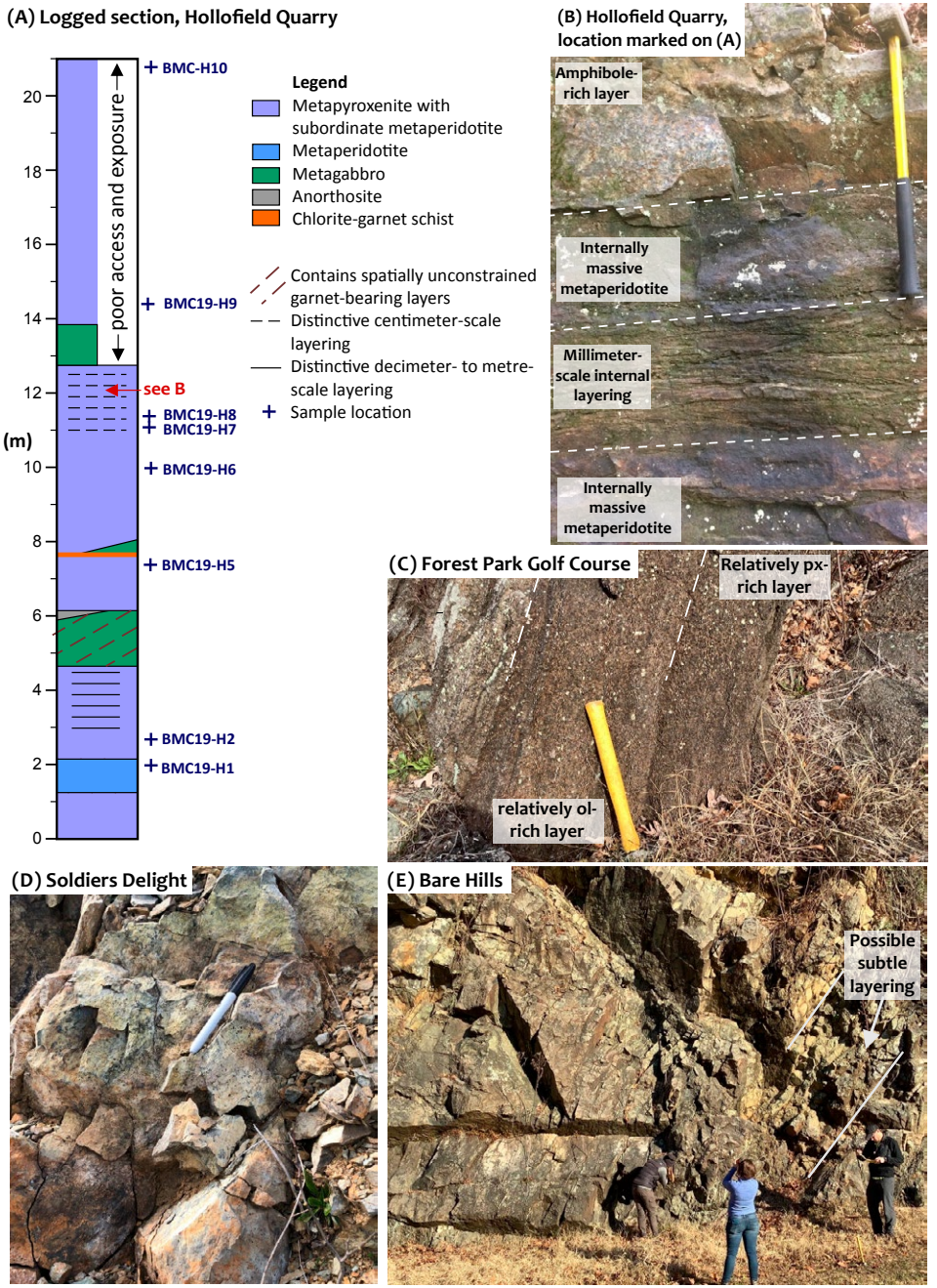

well-foliated L-S tectonites that contain lenticular, millimeter- to meter-scale pods of weakly deformed serpentinite separated by anastomosing mylonitic bands (Burgess et al., 2009).

SAMPLES AND FIELD RELATIONSHIPS

This study focuses on the ultramafic portions of the BMC in Baltimore and surrounding counties (referred to as the "Baltimore block" by Hanan and Sinha [1989]). A total of 19 samples of ultramafic rock were collected from the Hollofield Ultramafite (n = 12), Soldiers Delight Ultramafite (n = 5), and ultramafic body at Bare Hills (n = 2) between August and December 2019 (Fig. 1B). Of the 12 samples collected from the Hollofield Ultramafite, the majority of samples were taken from Hollofield Quarry (n = 8), with additional samples from Ashburton Reservoir (n = 3) and Forest Park Golf Course (n = 1; Fig. 1B). We note that the Ashburton Reservoir samples were collected following on-site excavation work as part of the ongoing Ashburton Tanks Project and were therefore not collected in situ. One Soldiers Delight sample (SD19-1) was collected from the entrance to the Choate chromite mine (Johnsson, 2017), but is not a sample of ore.

Hollofield Quarry—the best exposure of ultramafic rocks examined as part of this study—exposes crudely layered ultramafic and mafic rocks (Fig. 2A). There, serpentinized and amphibolitized ultramafic rocks (metapyroxenite with subordinate metaperidotite) are dominant, composing ~85% of the logged section, with mafic rocks (metagabbro and rare anorthosite) composing the remainder of the exposure. The contacts between the lithological units are generally sharp where observed and are commonly marked by notably more weathered

Figure 2. (A) Geologic log of the Hollofield Quarry exposure. Sample locations are marked. (B–E) Field photographs detailing the basic field characteristics of the studied rocks. Field photograph locations are as follows: B = 39.3095 °N / 76.7924 °W; C = 39.3225 °N / 76.7008 ° W; D = 39.4395 °N / 76.8315 °W; and E = 39.3872 °W / 76.6596 °W. Abbreviations: px—pyroxene; ol—olivine.

material. Metaperidotite units display centimeter-scale, discontinuous internal layering, whereas metapyroxenite units are massive, subtly layered at the centimeter scale or distinctly layered at the millimeter to centimeter scale (Fig. 2B). Metagabbro units are generally massive to subtly layered on the outcrop scale, with garnet restricted to rare, ~10-cm-thick layers. Distinctive, centimeter-scale layering of metapyroxenite and metaperidotite is also observed in smaller outcrops at Forest Park Golf Course in the eastern part of the Hollofield Ultramafite (e.g., Fig. 2C). In contrast, the serpentinites (after peridotite) at Soldiers Delight (Fig. 2D) and Bare Hills (Fig. 2E) are generally massive at the outcrop scale, although extremely subtle layering may be present on the scale of ~10 cm at Bare Hills. These field observations are consistent with previous field descriptions of the BMC (see Hanan and Sinha, 1989).

ANALYTICAL METHODS

Bulk-Rock Geochemistry

All samples analyzed for bulk-rock compositions were ground to a fine powder using the rock preparation facilities in the Department of Mineral Sciences at the Smithsonian Institution's National Museum of Natural History (Washington, D.C., USA). Weathered surfaces were removed using a diamond-bladed rock saw before samples were crushed using an agate jaw crusher and ground using an agate ring mill. Sample powders were then ignited at 900 °C for 2 h, with loss-on-ignition determined gravimetrically.

Major and Minor Elements

Ignited powders were subject to major element analysis using a Spectro-XEPOS benchtop X-ray fluorescence energy-dispersive spectroscopy (EDS) spectrometer in the Earth and Planets Laboratory, Carnegie Institution of Washington (D.C.). Laboratory protocols have been developed to analyze powdered samples (>0.2 g) from a wide range of ultramafic, mafic, and felsic lithologies. Accuracy was constrained by analyzing international reference materials W1 and DTS-1, with precision assessed by repeat analyses of the standards in different sample batches.

Trace Elements

For each sample, a sample mass of 0.5 g was weighed and mixed with 2.5 g of lithium tetraborate flux in a platinum crucible. The mixture was then fused over a Meker burner and quenched to a glass on a platinum mold. Glass fragments were mounted in epoxy and analyzed by laser ablation inductively coupled plasma mass spectrometry (LA-ICP-MS) using a Teledyne-Cetac Analyte G2 193 nm laser coupled to an Agilent 8900 quadrupole ICP-MS at Johns Hopkins University (Department of Earth and Planetary Sciences; Baltimore). To maximize analysis volume, minimize effects of potential sample heterogeneity, and minimize "down-hole" elemental fractionation during ablation, data were collected using 600-µm-long line scans. Prior to each analysis, the line was "pre-ablated" to remove surface contamination and a 15 s baseline was collected. Analyses were conducted using a scan rate of 20 µm/s, laser repetition rate of 20 Hz, circular-spot diameter of 50 µm, and a fluence of 3 J/cm^2. Integration times for each isotope were 0.08 s, resulting in a sweep time for all isotopes of 2.924 s (~10 measurements of each isotope per 30 s analysis). Data were processed using the trace element data reduction scheme of the commercially available program Iolite (version 4) using ^{43}Ca as an internal standard. Standard reference glasses NIST 612, NIST 610, BHVO, and W1 were measured after every nine unknown analyses. See Supplemental Material[1] for certified values. NIST 612 was used as the primary standard for data reduction. The other standards were used to assess data accuracy; the average value for each element in each glass was within 14% of its reported value. Each unknown was measured three times. The precision of unknown elemental concentrations (reported as the 2se [standard error] of each analysis; see the Supplemental Material) varies by analysis, but generally scales with concentration, for example: ±5%–15% at >2 ppm, and ±10%–50% at 0.1 ppm.

Mineral Chemistry and Element Maps

Quantitative mineral analyses and element mapping were conducted using a JEOL 8900 electron microprobe equipped with five wavelength-dispersive spectroscopy (WDS) detectors and one EDS detector at the Smithsonian Institution's National Museum of Natural History (Department of Mineral Sciences). For mineral analysis, the accelerating voltage was set to 20 kV, the beam current to 10 nA, and spot diameter to 1 µm. Calibration was conducted using a suite of Smithsonian standards, with separate secondary standards analyzed regularly to assess the accuracy of the analyses. The raw data, which are included in the Supplemental Material (footnote 1), were recalculated to element oxide percentages, with Fe^{2+} and Fe^{3+} calculated using the stoichiometric method of Droop (1987). For element mapping, the beam current was increased to 100 nA to ensure meaningful counts for minor elements, and a beam diameter of 1–2 µm was used, depending on the size of the map. The nominal smallest spot size of the beam is ~1 µm. However, sub-micron resolution was achieved by overlaying 1 µm analytical spots. Minor elements (V, Mn, Ti, Co, and Ni) were mapped using the WDS detectors, with major elements (Na, Mg, Al, Si, K, Ca, Cr, and Fe) mapped using the EDS detector.

RESULTS

Petrography

The ultramafic rocks from Hollofield Quarry, Ashburton Reservoir, and Forest Park Golf Course comprise olivine, serpentine, orthopyroxene, clinopyroxene, and amphibole in varying proportions, with accessory spinel and ilmenite present in almost all samples (Table 1; Figs. 3A–3D). Olivine generally shows near-complete alteration to

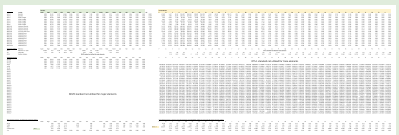

[1]Supplemental Material. Excel file containing bulk-rock and mineral chemical data, including standard data and precision calculations. Please visit https://doi.org/10.1130/GEOS.S.13477356 to access the supplemental material, and contact editing@geosociety.org with any questions.

TABLE 1. MODAL MINERAL PROPORTIONS FOR EACH OF THE SAMPLES ASSESSED AS PART OF THIS STUDY, BALTIMORE MAFIC COMPLEX

Sample	Latitude (°N)	Longitude (°W)	Locality	ol (mod%)	srp (mod%)	opx (mod%)	cpx (mod%)	am (mod%)	plg (mod%)	chl (mod%)	Accessory phase
BMC19-H1	39.3095	76.7924	Hollofield Quarry	2	63			35			spl, ilm
BMC19-H2	39.3095	76.7924	Hollofield Quarry			2		98			spl, ilm
BMC19-H5	39.3095	76.7924	Hollofield Quarry					100			spl, ilm
BMC19-H6	39.3095	76.7924	Hollofield Quarry	15	40	10	5	30			spl, ilm
BMC19-H7(1)	39.3095	76.7924	Hollofield Quarry	1	99						spl, ilm
BMC19-H7(2)	39.3095	76.7924	Hollofield Quarry	4				96			spl, ilm
BMC19-H8	39.3095	76.7924	Hollofield Quarry					100			spl, ilm
BMC19-H9	39.3095	76.7924	Hollofield Quarry					100			spl, ilm
BMC19-H10	39.3095	76.7924	Hollofield Quarry					100			spl, ilm
BMC19-A1	39.3228	76.6698	Ashburton Reservoir					100			spl
BMC19-A2	39.3228	76.6698	Ashburton Reservoir					100			
BMC19-A3	39.3228	76.6698	Ashburton Reservoir	2	1		37	60			
BMC19-G2	39.3225	76.7008	Forest Park Golf Course	8	50		12	20	6	4	
SD19-1	39.4126	76.8339	Soldiers Delight		100						spl
SD19-2	39.4203	76.8412	Soldiers Delight		100						spl
SD19-3	39.4203	76.8412	Soldiers Delight		100						spl
SD19-4	39.4395	76.8315	Soldiers Delight		100						
SD19-5	39.4395	76.8315	Soldiers Delight		100						spl
BH19-1	39.3872	76.6596	Bare Hills		60			40			spl
BH19-2	39.3872	76.6596	Bare Hills		80			20			spl

Note: Sample BMC19-H7 is distinctly layered, with modal mineral proportions gives for both layers sampled by the thin section. Abbreviations: ol—olivine; mod—modal; srp—serpentine; opx—orthopyroxene; cpx—clinopyroxene; am—amphibole; plg—plagioclase; chl—chlorite; spl—spinel; ilm—ilmenite.

serpentine (and associated magnetite), though relict grains occur as 0.2–0.8-mm-diameter anhedral remnants. In rare cases, where serpentinization is less pervasive (e.g., sample BMC19-H6; Fig. 1), olivine grains may be subhedral and 1.0–1.5 mm in diameter. Amphibole occurs as 0.1–8.0-mm-diameter anhedral to subhedral grains, with smaller (sub-millimeter-scale) grains common where amphibole appears to pseudomorph clinopyroxene, and larger grains more common in monomineralic samples (e.g., sample BMC19-A1). Sample BMC19-G2 is unique, displaying millimeter-scale rounded areas comprising plagioclase, extremely fine-grained chlorite, and amphibole (Fig. 3D).

All ultramafic rocks assessed from Soldiers Delight ($n = 5$) are serpentinites, comprising ~100% serpentine alongside accessory spinel group minerals (Fig. 3E). Spinel occurs as 0.03–1.5-mm-diameter grains that are generally subhedral (Table 1). The ultramafic rocks from Bare Hills ($n = 2$) comprise (in modal percent) 60%–80% serpentine and 20%–40% amphibole, alongside accessory spinel group minerals (Table 1; Fig. 3F). Amphibole occurs as 0.1–2.5-mm-diameter grains that are anhedral to subhedral, with larger grains generally elongate and smaller grains representing pseudomorphs after clinopyroxene. Spinel is generally subhedral to anhedral and <6 mm in diameter, with distinct rims observable with the naked eye. Based on the thin sections assessed here ($n = 7$), the Soldiers Delight and Bare Hills ultramafic rocks appear distinct from the Hollofield Quarry, Ashburton Reservoir, and Forest Park Golf Course ultramafic rocks in terms of their modal mineral proportions (see Table 1).

Bulk-Rock Geochemistry

Figures 4–6 detail the geochemical characteristics of the ultramafic rocks analyzed as part of this study. Table 1 provides specific sample locations and the modal mineralogy for each sample. The full bulk-rock geochemical data set is included in the Supplemental Material (footnote 1). Throughout the following sections, the presented data are compared to those of residual mantle rocks from the Oman ophiolite and abyssal peridotites (Godard et al., 2000, 2008; Paulick et al., 2006).

Major and Minor Elements

Hollofield Quarry samples contain (in weight percent unless stated): 23%–33% MgO, 41%–57%

SiO_2, <0.2% TiO_2, 1%–2.7% Al_2O_3, 6%–22% Fe_2O_3, 2%–9% CaO, <0.2% Na_2O, 169–1288 ppm Ni, and 920–6220 ppm Cr (Fig. 4). As shown on the bulk-rock bivariate plots included in Figure 4, MgO in the ultramafic rocks displays moderate negative correlations (R^2 = 0.4–0.7) with Al_2O_3 and SiO_2, weak negative correlations (R^2 = 0.1–0.4) with TiO_2, CaO, and Na_2O, a weak positive correlation with Fe_2O_3 and Ni, and no correlation with Cr. Data for these samples exhibit limited overlap with the literature data for residual mantle rocks (ophiolites and abyssal peridotites) on the major and minor element bivariate plots shown in Figure 4.

Relative to the Hollofield Quarry samples (Fig. 4), the Ashburton Reservoir samples are relatively poor in MgO (16.8–17.5 wt%) and rich in TiO_2 (0.2–0.3 wt%), Al_2O_3 (2.5–6.5 wt%), CaO (13–18 wt%), and Na_2O (<0.5 wt%). However, these rocks show significant overlap with the Hollofield Quarry samples for all other major and minor elements (Fig. 4), including SiO_2 (53–55 wt%). The one sample from the Forest Park Golf Course contains 28 wt% MgO and falls within the ranges defined by the Ashburton Reservoir and Hollofield Quarry samples for most other major and minor elements. Data for these Ashburton and Forest Park samples show no overlap with the literature data for residual mantle rocks on major and minor element bivariate plots.

The analyzed rocks from Soldiers Delight and Bare Hills are considerably more MgO rich than the Hollofield Ultramafite samples, containing 41–44 wt% MgO. These samples form tight clusters on most major and minor element bivariate plots (Fig. 4), containing (in weight percent unless stated): 44%–51% SiO_2, <0.1% TiO_2, <0.4% Al_2O_3, 6%–7% Fe_2O_3, <7% CaO, 183–2542 ppm Ni, and 217–3165 ppm Cr. These samples collectively show significant overlap with the field for residual mantle rocks on all major and minor element bivariate plots in Figure 4.

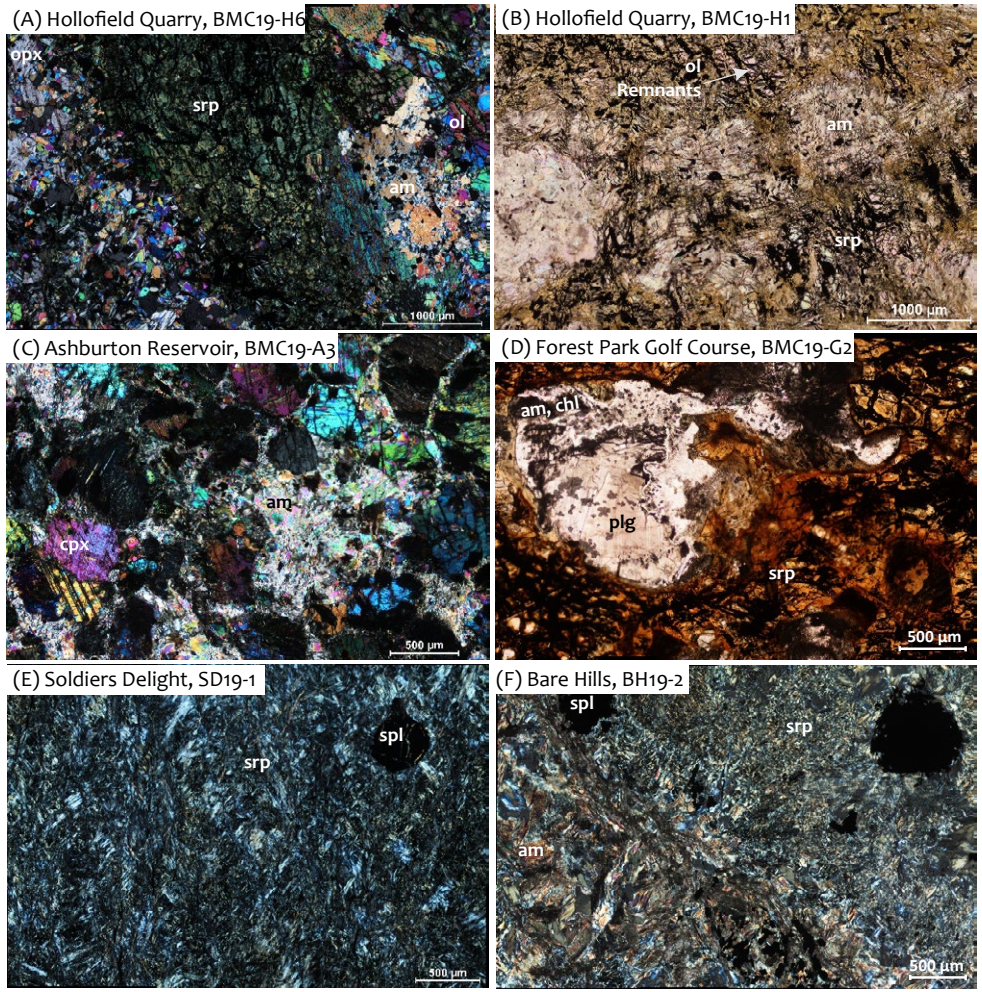

Figure 3. Photomicrographs detailing the basic mineralogy and textural characteristics displayed by the ultramafic rocks assessed as part of this study. Photomicrographs A, C, E, and F were taken using cross-polarized light, while B and D were taken using plane-polarized light. Abbreviations: am—amphibole; chl—chlorite; cpx—clinopyroxene; ol—olivine; opx—orthopyroxene; plg—plagioclase; spl—spinel; srp—serpentine.

Trace Elements

Trace element bivariate plots (Fig. 5) indicate that a broad suite of elements, including Rb, Ba, Th, Nb, La, Ce, and Sr, in the Hollofield Quarry ultramafic rocks show little to no correlation with Yb (R^2 ≤0.15). In contrast, other elements, such as Zr, Sm, Ti, Gd, Y, Ho, and Lu, all show moderate to strong positive correlations (R^2 ≥0.50) with Yb, while Nd shows a poor correlation (R^2 = 0.21). Discussion of these data—and the implications for element mobility—is included in the Bulk-Rock Element Mobility section, and likely mobile elements are highlighted in red in Figure 6.

On chondrite-normalized rare-earth element (REE) plots, the ultramafic samples from Hollofield Quarry generally show flat patterns ($[La/Lu]_N$ = 0.3–1.1; Fig. 6A) with some weak negative Eu

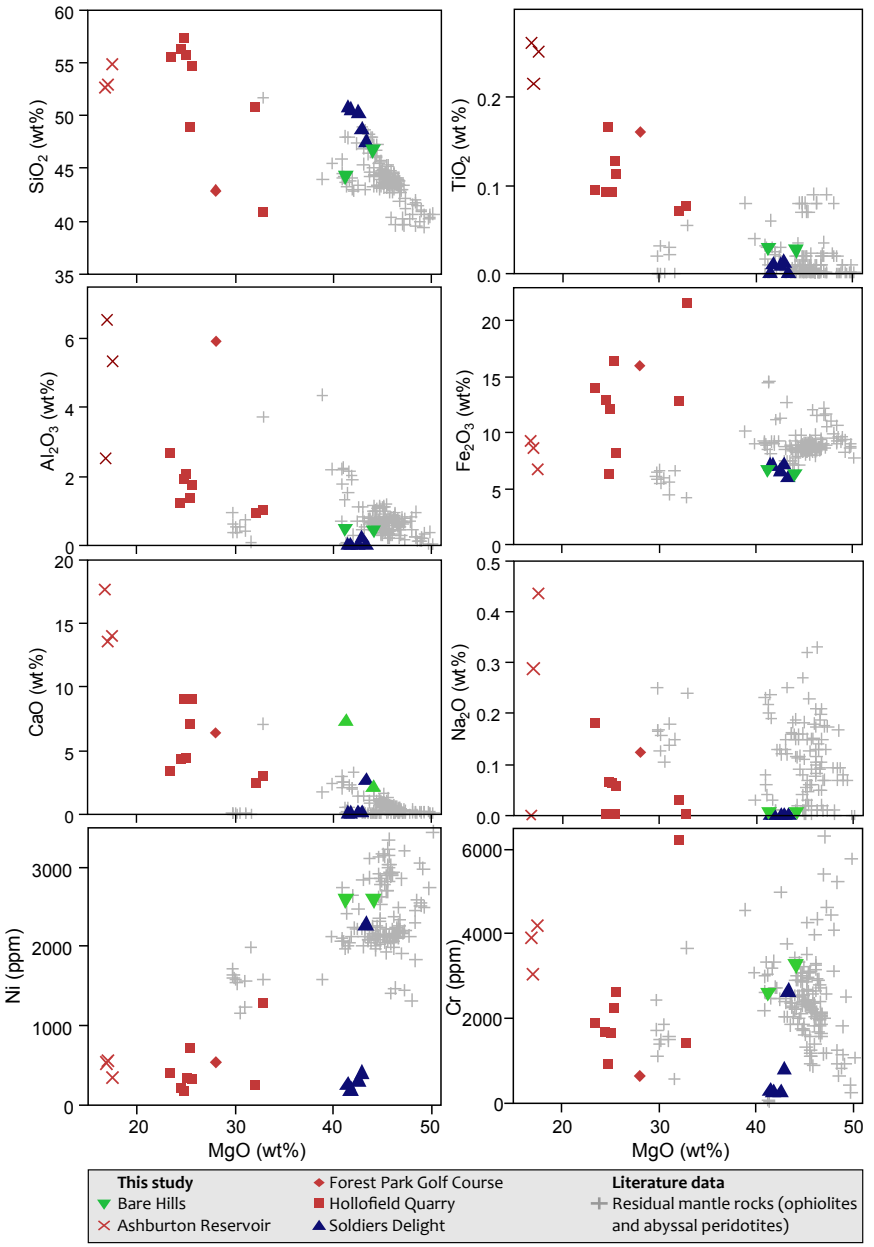

Figure 4. Major and minor element bivariate plots for the ultramafic rocks from the Baltimore Mafic Complex analyzed in this study. Literature data are from Godard et al. (2008, 2000) and Paulick et al. (2006).

anomalies and normalized values ranging from 0.3 to 2.3. One sample shows relative light-REE (LREE) enrichment ($[La/Sm]_N = 8$) but is otherwise broadly comparable to the other samples from this locality. On primitive mantle–normalized trace element plots, these samples show subtly U-shaped patterns, alongside weak positive Ti anomalies and some negative Nb anomalies (Fig. 6E). The most compatible elements show mildly positive slopes ($[Zr/Yb]_N = 0.1–0.3$), while the most incompatible elements show mildly to moderately negative slopes ($[Rb/Zr]_N = 3–32$). There is almost no overlap with the field for residual mantle rocks (shown in gray in Fig. 6).

On chondrite-normalized REE plots, the ultramafic samples from Ashburton Reservoir and the Forest Park Golf Course show broadly flat patterns ($[La/Lu]_N = 0.4–1.9$), mild negative heavy-REE (HREE) slopes ($[Gd/Lu]_N = 1.0–1.3$), weak positive LREE slopes ($[La/Sm]_N = 0.4–0.6$), and normalized REE contents ranging 1.1–6.8 (Fig. 6B). One sample displays weak negative LREE patterns ($[La/Sm]_N = 1.6$) but is otherwise comparable to the other samples from these localities. On primitive mantle–normalized trace element plots, these samples show overall flat patterns ($[Nb/Yb]_N = 0.2–0.9$), with negative Zr-Hf-Th-U anomalies, flat compatible-element patterns ($[Sm/Yb]_N = 0.8–1.2$), and weak negative Ti anomalies (Fig. 6F). These samples show almost no overlap with the field for residual mantle rocks on these plots (Figs. 6B, 6F). The patterns are broadly parallel to those of the samples from Hollofield Quarry, but exhibit relative enrichment relative to these samples (Figs. 6B, 6F).

As illustrated by the chondrite-normalized REE plot, the ultramafic rocks from Soldiers Delight are depleted in most REEs (Fig. 6C), showing generally flat HREE patterns ($[Gd/Lu]_N = 0.7–0.9$), negatively sloping LREE patterns ($[La/Sm]_N = 4.5–6.0$), and normalized values ranging from 0.004 to 0.7. One sample shows negatively sloping HREE patterns ($[Gd/Lu]_N = 2.0$) but is otherwise comparable to the other Soldiers Delight ultramafic rocks. The overall REE concentrations are similar to those of residual mantle rocks, although they exhibit a weak negative rather than positive chondrite-normalized REE slope (Fig. 6C). On primitive mantle–normalized

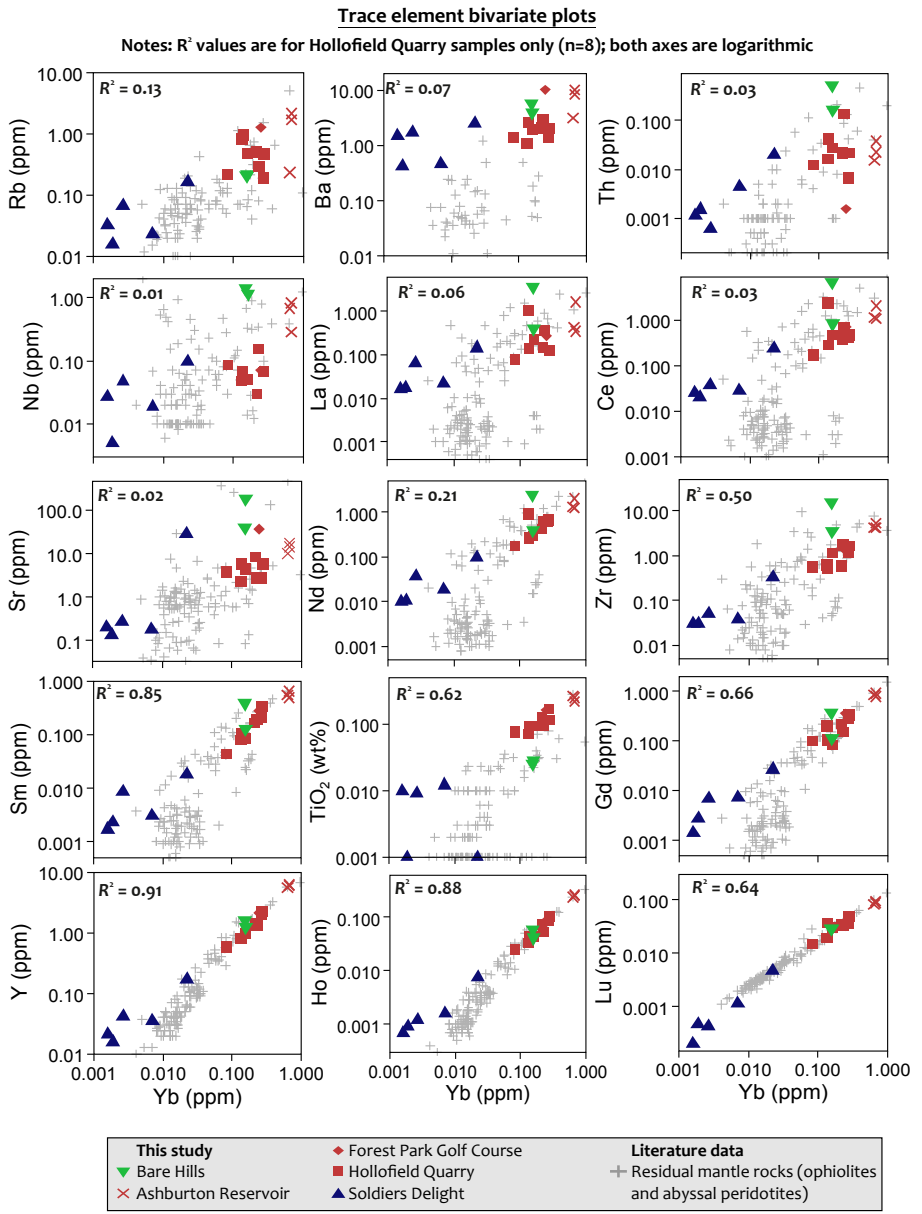

Figure 5. Trace element bivariate plots for the ultramafic rocks from the Baltimore Mafic Complex analyzed in this study. Literature data are from Godard et al. (2008, 2000) and Paulick et al. (2006).

trace element plots, these samples show slight U-shaped patterns, with positively sloping patterns for the most compatible elements ($[Zr/Yb]_N$ = 0.2–0.8), negatively sloping patterns for the most incompatible elements ($[Rb/Zr]_N$ = 8–24), and positive Ti anomalies (Fig. 6G). There is near-complete overlap with the field for residual mantle rocks for all samples, with some enrichment in U and LREEs and some minor depletion in the most compatible elements relative to this field. Notably, the positive Ti anomalies shown by the Soldiers Delight rocks correlate with those shown for residual mantle rocks.

On chondrite-normalized REE plots, the ultramafic rocks from Bare Hills show relatively flat HREE patterns ($[Gd/Lu]_N$ = 0.5–1.6), negatively sloping LREE patterns ($[La/Sm]_N$ = 1.8–5.6), and normalized abundances ranging from 0.3 to 12.2 (Fig. 6D). On primitive mantle–normalized trace element plots (Fig. 6H), these samples show broad negative slopes ($[Nb/Yb]_N$ = 4.3–5.2) except for depletion in the most incompatible elements ($[Rb/Nb]_N$ = 0.2). One sample shows prominent negative Eu and Ti anomalies and a weak negative Sr anomalies; the other shows weak negative Eu and Ti anomalies and a large positive Sr anomaly (Fig. 6H). Neither sample composition overlaps with the field for residual mantle rocks (Figs. 6D, 6H).

Spinel Mineral Chemistry

A total of 761 quantitative analyses were conducted on spinel-group mineral grains from the Ashburton Reservoir (*n* = 62), Hollofield Quarry (*n* = 377), Soldiers Delight (*n* = 185), and Bare Hills (*n* = 137) localities. While these analyses indicate the assessed minerals are largely not spinel *sensu stricto*, we hereafter refer to all spinel-group minerals as such. Spinel assessed ranges from 7 to 3600 µm in diameter and can be broadly subdivided into four petrographic groups (Table 2; Fig. 7):

- ***Type 1: Distinctly zoned spinel***, wherein zonation is apparent in back-scattered electron (BSE) images and chemical maps (Figs. 7A–7C) and with the naked eye in hand specimen. Cores are generally homogenous and euhedral,

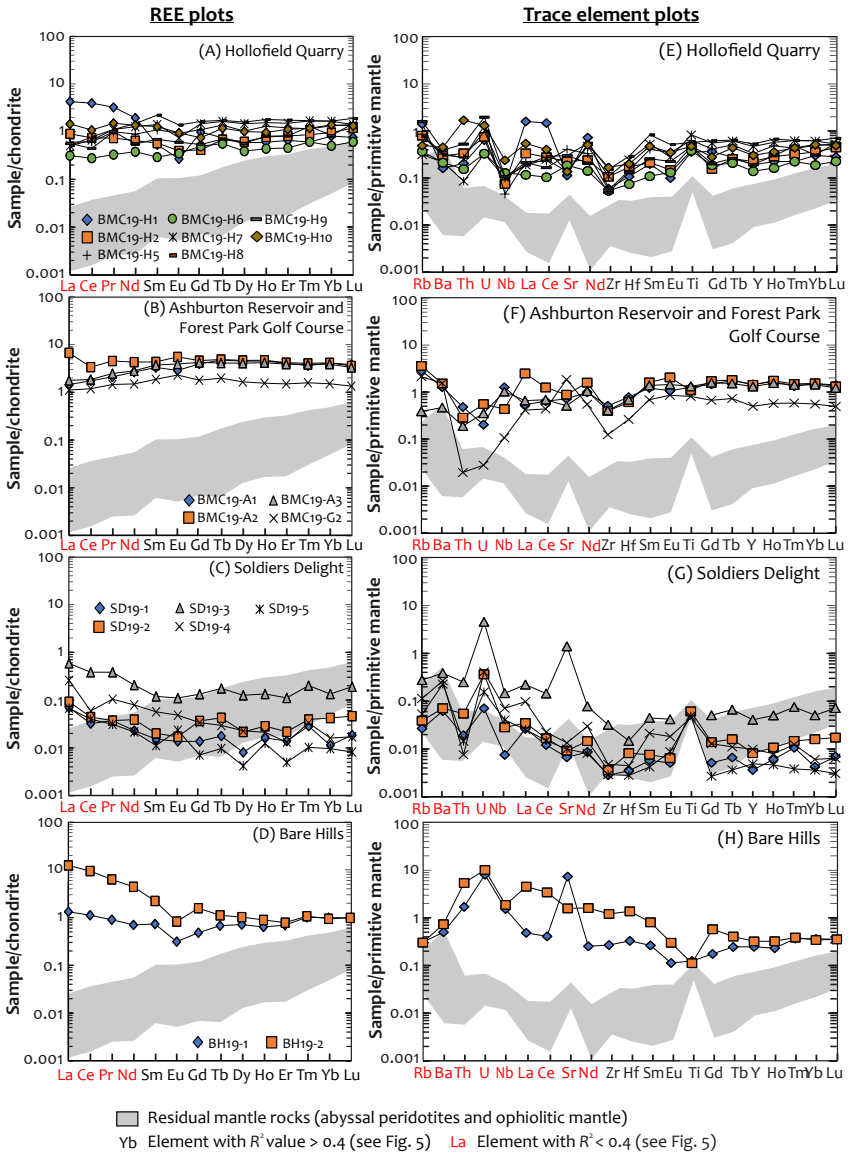

Figure 6. Chondrite-normalized rare earth element (REE) (A–D) and primitive mantle–normalized trace element (E–H) plots for the ultramafic rocks from the Baltimore Mafic Complex analyzed in this study. Elements highlighted in red likely experienced mobility during metamorphism and alteration. See the Bulk-rock Element Mobility section for full details. Literature data are from Godard et al. (2008, 2000) and Paulick et al. (2006). Normalizing values are after McDonough and Sun (1995).

and the transition from cores to rim is sharp (a few tens of micrometers or less). The type 1 rims are commonly thick relative to the size of the grains, are concentrically zoned with respect to the concentration of some elements (Figs. 7A–7C) and tend to be more inclusion rich in their outermost regions.

- ***Type 2: Cryptically zoned spinel***, wherein zonation is significantly less marked than type 1, gradational, and apparent only in chemical maps (Figs. 7D–7F). Unlike the type 1 spinel, type 2 spinel does not contain distinct core-rim compositional boundaries, although grains do exhibit progressive changes in the concentration of some elements toward the edges of grains. Specifically, relative to cores, the rims of type 2 spinel show relative enrichment in Fe and relative depletion in Cr, Mn, and Ti. The outmost regions are invariably inclusion rich (Fig. 7D). In rare cases, small, chemically distinct zones occur in the cores of grains, although these areas are barely visible in BSE images (e.g., Figs. 7D–7F).
- ***Type 3: Homogenous spinel***, wherein the chemical composition is consistent throughout individual grains (Figs. 7G–7H).
- ***Type 4: Partially rimmed spinel***, wherein the composition is generally homogenous, but an extremely thin, Fe-rich rim (<10 µm thick) occurs on one or more sides of individual grains (Figs. 7I–7J).

The type 1 (distinctly zoned) and type 2 (cryptically zoned) spinel grains are relatively large, showing mean diameters of 1016 µm and 760 µm, respectively. Comparatively, type 3 (homogenous) and type 4 (partially rimmed) spinel grains are small, exhibiting mean diameters of 140 µm and 154 µm, respectively. Small silicate veins that crosscut larger spinel grains are ubiquitous but rarely display any spatial correlation with the composition of spinel (Figs. 7A–7F). Where spinel is altered in association with the veins (Figs. 7K–7L), it is defined by compositions that are relatively rich in Fe, Si, and K and poor in Cr and V (Table 3).

As summarized in Table 2, there is significant variation in the petrographic types of spinel observed at different localities. Spinel grains from

TABLE 2. PETROGRAPHIC CLASSIFICATION OF THE QUANTITATIVE SPINEL ANALYSES FROM THE STUDIED LOCALITIES, BALTIMORE MAFIC COMPLEX

Locality	Total spinel grains (*N*)	Type 1: Distinctly zoned spinel grains (*n*)	Type 2: Cryptically zoned spinel grains (*n*)	Type 3: Homogeneous spinel grains (*n*)	Type 4: Partially rimmed spinel grains (*n*)	Vein-altered analyses (*n*)	Mean diameter
Ashburton Reservoir	62	n/a	n/a	62	n/a	n/a	93 µm
Hollofield Quarry	377	n/a	n/a	339	36	2	132 µm
Soliders Delight	185	66 core + 62 rim	33	6	n/a	18	497 µm
Bare Hills	137	20 core + 37 rim	57	23	n/a	n/a	1376 µm
Mean diameter	761	1016 µm	760 µm	140 µm	154 µm	n/a	n/a

Note: The Forest Park Golf Course sample (BMC19-G2) does not contain spinel. n/a—no data for this classification.

Ashburton Reservoir and Hollofield Quarry generally classify as type 3 (homogenous) spinel, with a small number of type 4 (partially rimmed) spinel grains also present. In contrast, spinel grains analyzed from Soldiers Delight and Bare Hills generally classify as type 1 (distinctly zoned) or type 2 (cryptically zoned), with a small number of type 3 (homogenous) spinel grains (Table 2).

The succeeding text summarizes the broad characteristics of this large data set, with Table 3 providing a detailed overview of the geochemical characteristics displayed by each petrographic group in each locality. Minimum, maximum, and mean values are provided for every element analyzed, as well as for the following key geochemical proxies (Barnes and Roeder, 2001): $Fe^{2+}\#$ ($Fe^{2+}/[Fe^{2+} + Mg]$), $Fe^{3+}\#$ ($Fe^{3+}/[Cr + Al + Fe^{3+}]$) and Cr# ($Cr/[Cr + Al] \times 100$). The cations per formula unit values are provided in the Supplemental Material (footnote 1). Figure 8 illustrates the relative composition of the analyzed spinel using the $Fe^{2+}\#$ versus $Fe^{3+}\#$ and $Fe^{3+}\#$ versus TiO_2 plots, with associated elemental maps included for petrographic context.

The cores of type 1 (distinctly zoned) spinel grains from both Soldiers Delight and Bare Hills, which classify as chromite, are relatively homogenous in their major and minor element compositions (Table 3; Figs. 8A–8B). Compared with other spinel types assessed here, they exhibit relatively high MgO (5.0–8.4 wt%), Cr_2O_3 (50.8–59.4 wt%), and Al_2O_3 (6.1–12.2 wt%) contents and distinctly low Fe_2O_3 abundances (0.4–4.2 wt%). On $Fe^{2+}\#$ versus $Fe^{3+}\#$ and $Fe^{3+}\#$ versus TiO_2 plots, the cores of type 1 spinel plot as a tight, isolated group. The rims of type 1 spinel, which classify as chromite, Fe-chromite, Cr-magnetite, and magnetite, are compositionally zoned, with Cr_2O_3 (3.5–46.5 wt%), TiO_2 (<1.0 wt%), and Fe_2O_3 (8.6–60.1 wt%) showing moderate to large ranges (Table 3). Cr# and $Fe^{2+}\#$ are extremely high, and $Fe^{3+}\#$ shows broad ranges. As illustrated in Figures 8A–8B, these zoned rim compositions form a systematic array away from innermost rim compositions.

Type 2 (cryptically zoned) spinel grains from both Soldiers Delight and Bare Hills, which classify as chromite, Fe-chromite, Cr-magnetite, and magnetite, show wide ranges for TiO_2 (<1.7 wt%), Cr_2O_3 (0.3–55.9 wt%), and Fe_2O_3 (1.7–66.2 wt%; Table 3). Narrower ranges are observed for other elements, such as MgO and Al_2O_3. $Fe^{2+}\#$ are high, while Cr# and $Fe^{3+}\#$ show moderate to large ranges. These compositions also define systematic core-rim arrays on the $Fe^{2+}\#$ versus $Fe^{3+}\#$ and $Fe^{3+}\#$ versus TiO_2 plots (Figs. 8E–8F), with these arrays overlapping with the array shown by the type 1 spinel rims.

Type 3 (homogenous) spinel grains from Bare Hills and Soldiers Delight, which classify as Fe-chromite, Cr-magnetite, and magnetite, show broad ranges in Cr_2O_3 (0.5–12.7 wt%), FeO (30.8–40.0 wt%), and Fe_2O_3 (44.8–66.5 wt%) contents and a tight range in TiO_2 (<0.3 wt%; Table 3; Figs. 8E–8F). This group of spinel records high Cr#, $Fe^{2+}\#$, and $Fe^{3+}\#$ (Table 3), forming broad arrays on the Fe^{2+} versus Fe^{3+} and Fe^{3+} versus TiO_2 plots (Figs. 8A–8B). Compositionally, type 3 spinel from Ashburton Reservoir and Hollofield Quarry is comparable to that of Bare Hills, although these analyses show significant enrichment in TiO_2 (Table 3), as detailed in Figure 8F. Type 3 arrays for the Ashburton Reservoir and Hollofield Quarry samples also form broad, similarly oriented arrays on bivariate plots (Figs. 8E–8F), but there is offset between these arrays and those of the Bare Hills and Soldiers Delight samples (Figs. 8E–8F).

The cores of type 4 (partially rimmed) spinel, which classify as Cr-magnetite and magnetite, show tight ranges in their major and minor element compositions, with relatively high TiO_2 (2.5–3.1 wt%), moderately high Cr_2O_3 (33.4–35.8 wt%), and relatively low Fe_2O_3 (12.8–14.5 wt%; Table 3). $Fe^{3+}\#$ is low, whereas Cr# and $Fe^{2+}\#$ are high. In contrast, the rims of the type 4 spinel show broader compositional ranges, alongside relative enrichment in Fe_2O_3 (53.9–65.7 wt%) and relative depletion in Cr_2O_3 (1.3–7.8 wt%; Table 3). Core analyses plot as a tight, isolated group on $Fe^{2+}\#$ versus $Fe^{3+}\#$ and $Fe^{3+}\#$ versus TiO_2 plots, whereas rim analyses show significant overlap with type 3 compositions (Figs. 8E–8F).

DISCUSSION

Effects of Metamorphism and Hydrothermal Alteration

Bulk-Rock Element Mobility

The relative mobility of individual trace elements can be tested by plotting their concentrations against those of the most immobile elements (e.g., Zr, Y, and Yb) and determining the R^2 value (e.g.,

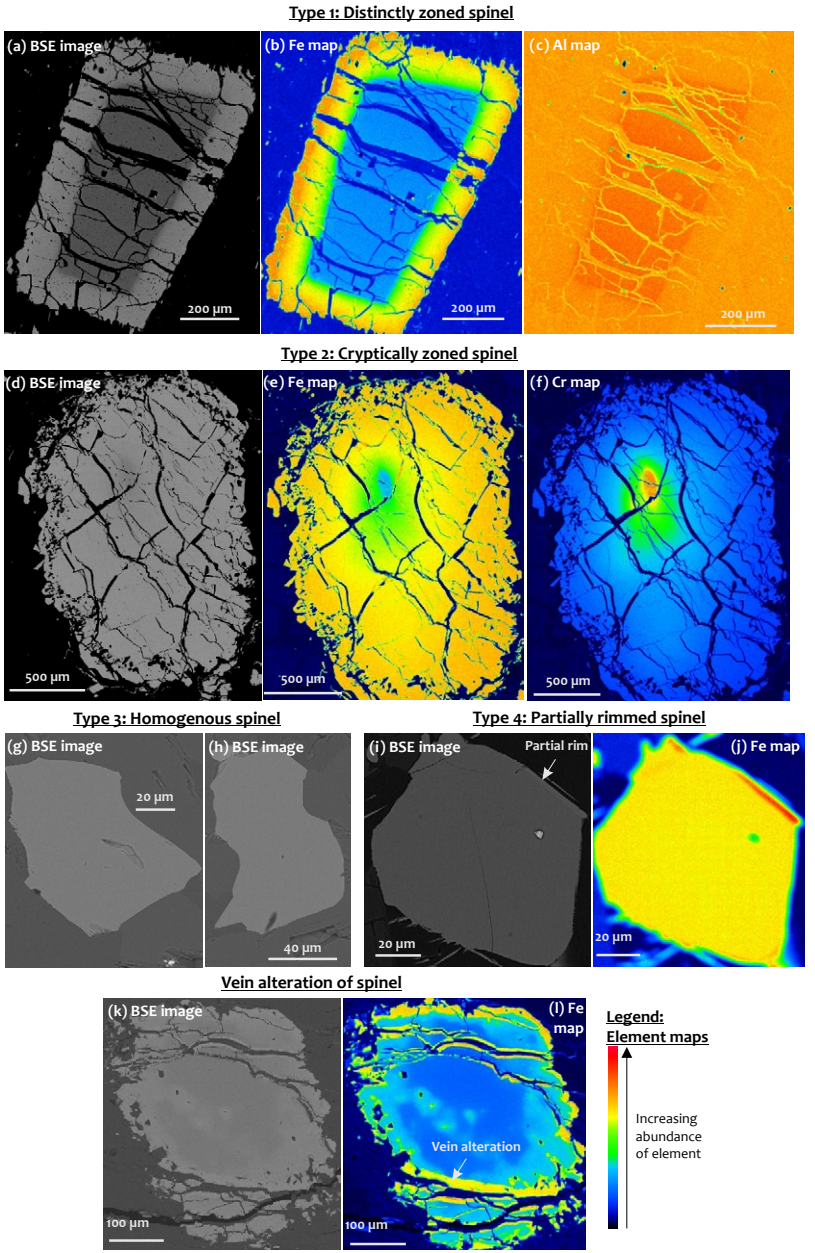

Figure 7. Back-scattered electron (BSE) images and chemical maps detailing the petrographic and basic chemical characteristics of the spinel grains assessed as part of this study. See Tables 2–3 and text for discussion.

Guice, 2019). All samples included must be cogenetic, with the reliability of such tests greater when utilizing large, well-characterized data sets (e.g., Guice et al., 2018, 2019). Because the BMC is poorly exposed, such an approach is not possible for all localities studied, but the demonstrably cogenetic and relatively well-exposed Hollofield Quarry samples (Figs. 2A–2B) can be utilized to test element mobility. While this method cannot elucidate the *specific* metasomatism experienced by every locality studied here (Hollofield Ultramafite, Hollofield Quarry, Bare Hills), it provides the best possible approximation.

As shown by the high R^2 values for Zr, Sm, Ti, Gd, Y, Ho, and Lu (when plotted against Yb; $R^2 \geq 0.5$; Fig. 5), these elements likely record limited mobility in the Hollofield Quarry rocks. In contrast, a large suite of elements, including Rb, Ba, Th, Nb, La, Ce, Sr, and Nd, show extremely poor correlations with Yb ($R^2 \leq 0.13$; Fig. 5). While some of these elements (e.g., Rb, Ba, and Sr) are typically considered mobile, others (e.g., Th, La, Ce, Nd, and Nb) are typically considered immobile. This is consistent with research suggesting that these elements (notably the LREEs) can be mobilized during some forms of hydrothermal alteration, particularly in ultramafic rocks that have experienced high-grade metamorphism and/or metasomatism (e.g., Wood, 1990; Yaxley et al., 1991; Lahaye et al., 1995; Powell et al., 2004; Guice et al., 2018, 2019). Moreover, the ultramafic rocks—particularly those from Soldiers Delight—display exceptionally low trace element concentrations, meaning that they have a high susceptibility to even small amounts of metasomatism via fluid and/or rock interactions.

These data indicate that there has been significant mobilization of Rb, Ba, Sr, the LREEs, Th, and possibly Nb associated with metamorphism and hydrothermal alteration of the Hollofield Quarry ultramafic rocks. While these metamorphic and metasomatic effects should not be immediately extrapolated to other localities investigated as part of this study, it is likely that a similar suite of elements experienced mobility during hydrothermal alteration. Given the higher modal abundances of secondary minerals (e.g., serpentine and amphibole) shown by the Soldiers Delight and Bare Hills

TABLE 3. GEOCHEMICAL CHARACTERISTICS OF THE SPINEL TYPES ANALYZED FROM EACH LOCALITY, BALTIMORE MAFIC COMPLEX

		Ash.	Hollofield Quarry			Soldiers Delight				Bare Hills				
Classification		3	3	4-c	4-r	1-c	1-r	2	3	1-c	1-r	2	3	Alt.
Number of grains		62	339	29	7	66	62	33	6	20	37	57	23	20
Major elements (wt%)														
MgO	Min.	0.04	0.04	0.75	0.01	5.04	0.52	0.29	0.25	5.11	1.50	1.30	1.13	0.10
	Max.	0.37	1.10	0.99	0.10	6.34	2.03	5.15	0.35	8.41	3.50	5.50	1.95	1.23
	Mean	0.15	0.31	0.90	0.06	5.50	1.07	1.83	0.30	7.25	2.39	2.40	1.57	0.46
Al_2O_3	Min.	0.03	0.01	0.34	0.01	7.20	n.d.	n.d.	n.d.	6.08	0.01	0.01	n.d.	n.d
	Max.	0.14	0.81	0.69	0.08	12.22	0.97	9.00	0.04	11.14	0.64	0.51	0.05	0.48
	Mean	0.06	0.18	0.49	0.03	8.96	0.06	1.35	<0.01	9.00	0.10	0.08	0.03	0.04
SiO_2	Min.	n.d.	n.d.	n.d.	0.05	n.d.	n.d.	n.d.	0.01	n.d.	n.d.	n.d.	n.d.	0.15
	Max.	0.04	0.76	0.05	0.3	0.18	1.15	0.06	0.07	0.80	0.11	0.72	0.07	1.95
	Mean	0.02	0.05	0.02	0.18	<0.01	0.02	0.01	0.03	0.08	0.04	0.05	0.03	0.84
TiO_2	Min.	0.22	0.34	2.48	0.08	n.d.	0.06	n.d.	n.d.	n.d.	0.03	0.05	0.04	n.d.
	Max.	2.64	5.56	3.07	0.54	0.11	0.37	0.32	0.09	0.09	0.95	1.64	0.23	0.08
	Mean	1.08	2.15	2.89	0.20	0.02	0.19	0.11	0.03	0.04	0.37	0.35	0.11	< 0.01
Cr_2O_3	Min.	3.73	0.23	33.44	1.30	52.73	3.45	0.32	0.45	50.81	5.10	5.55	2.80	1.33
	Max.	17.43	35.84	35.77	7.79	59.44	20.47	55.85	1.66	58.36	46.47	42.40	12.74	7.66
	Mean	8.05	9.71	34.87	3.40	56.74	12.00	29.58	0.77	55.30	16.10	15.64	6.41	3.17
MnO	Min.	0.01	n.d.	0.36	n.d.	0.43	n.d.	n.d.	n.d.	0.53	0.11	0.03	0.03	0.06
	Max.	1.30	0.61	0.64	0.12	0.85	0.59	0.79	0.11	1.25	0.82	2.03	0.31	2.74
	Mean	0.43	0.20	0.49	0.03	0.64	0.22	0.44	0.03	0.87	0.40	0.43	0.18	0.76
FeO	Min.	34.74	31.61	42.94	32.73	23.82	33.41	27.74	30.82	21.08	34.11	34.78	32.52	31.21
	Max.	43.85	44.98	44.52	39.19	27.97	42.66	41.68	31.99	31.18	42.84	43.82	40.02	39.62
	Mean	38.44	40.09	44.05	35.03	26.29	39.10	39.95	31.28	24.68	38.64	34.78	35.19	35.39
Fe_2O_3	Min.	31.44	12.34	12.82	53.92	0.36	30.20	1.66	64.02	0.90	8.56	9.75	44.77	47.44
	Max.	59.00	65.42	14.51	65.66	1.80	60.10	66.17	66.48	4.17	56.02	55.82	60.83	63.75
	Mean	49.72	44.40	13.48	61.41	1.16	45.44	28.11	65.73	1.89	39.08	39.85	54.55	58.60
NiO	Min.	n.d.	n.d.	n.d.	n.d.	n.d.	0.05	n.d.	0.48	n.d.	0.13	0.26	0.46	n.d.
	Max.	0.39	0.22	0.11	0.04	0.45	1.08	0.95	0.60	0.46	1.34	1.23	1.08	0.63
	Mean	0.08	0.07	0.03	0.01	0.05	0.76	0.37	0.54	0.13	0.75	0.77	0.84	0.06
Key geochemical proxies														
Cr#	Min.	98.54	84.6	97.4	95.7	75.0	98.8	80.9	91.2	77.9	98.1	98.4	98.7	93.1
	Max.	99.53	99.9	100.0	99.9	84.5	100.0	100.0	100.0	85.7	99.8	99.9	100.0	100.0
	Mean	99.08	97.7	98.1	98.8	81.1	99.7	96.3	98.0	80.8	99.4	99.4	99.4	99.3
Fe^{2+}#	Min.	0.98	0.95	0.96	0.99	0.68	0.92	0.75	0.97	0.58	0.85	0.76	0.88	0.91
	Max.	1.00	1.00	0.97	1.00	0.75	0.97	0.98	0.98	0.77	0.92	0.93	0.93	0.99
	Mean	0.99	0.98	0.96	1.00	0.73	0.95	0.91	0.98	0.65	0.88	0.88	0.91	0.97
Fe^{3+}#	Min.	0.59	0.23	0.23	0.84	0.00	0.51	0.02	0.97	0.01	0.14	0.16	0.73	0.81
	Max.	0.92	0.99	0.27	0.97	0.02	0.93	0.99	0.99	0.05	0.89	0.88	0.94	0.97
	Mean	0.82	0.77	0.25	0.93	0.01	0.74	0.44	0.09	0.02	0.65	0.66	0.86	0.93

Note: Cr# = molar Cr/[Cr/Al] x 100; Fe2+# = molar Fe2+/[Mg+Fe2++Fe3+]; Fe3+# = molar Fe3+/[Cr+Al+Fe3+]. Abbreviations: Ash.–Ashburton Reservoir; c—core; r—rim; Alt.—vein-altered spinel composition; Min.—minimum; Max.—maximum. Spinel classifications are as in Figure 7 and Table 2. See Supplemental Material (text footnote 1) for cations per formula unit values. n.d.—not detected.

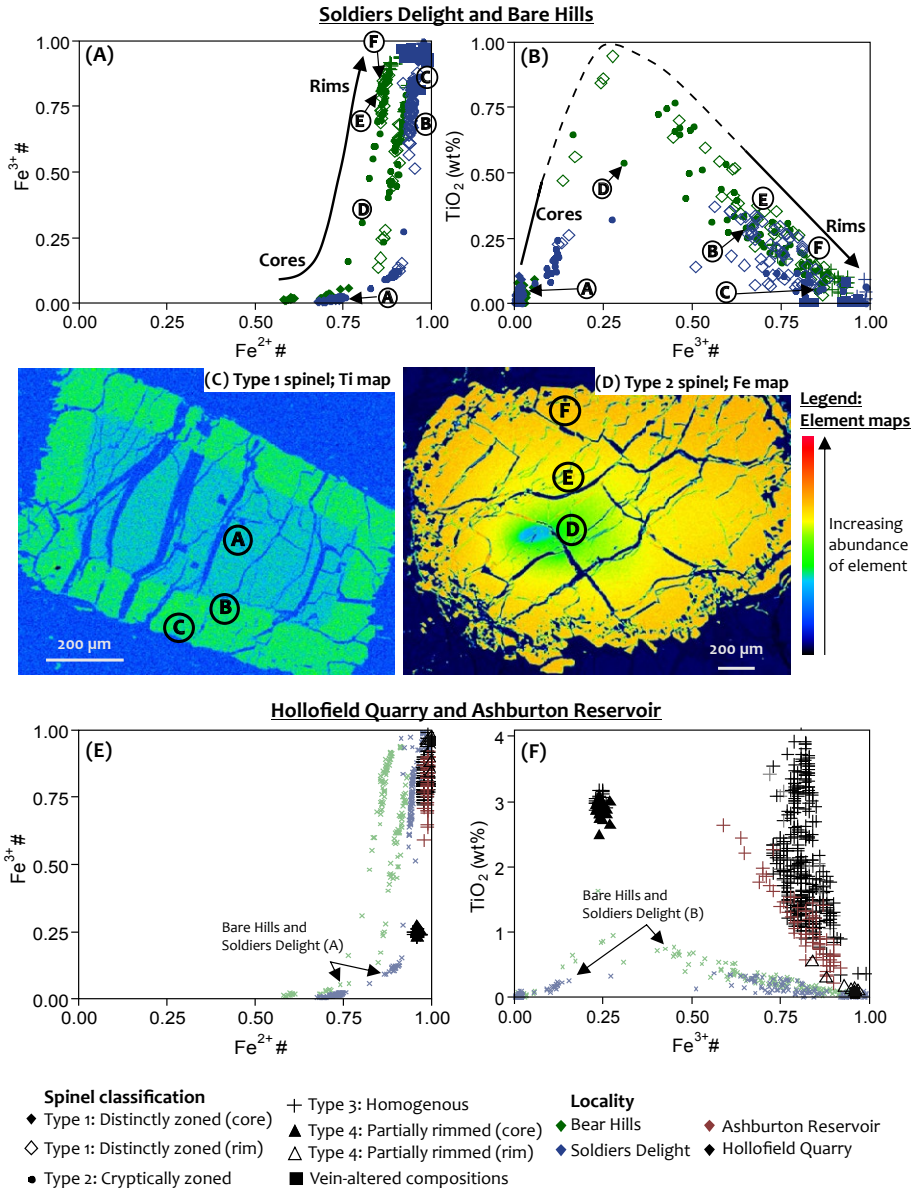

Figure 8. Bivariate plots and chemical maps detailing the compositions of spinel grains assessed as part of this study. Data from A and B are included in E and F for reference. Fe^{2+}# = molar $Fe^{2+}/[Mg+Fe^{2+}+Fe^{3+}]$; Fe^{3+}# = molar $Fe^{3+}/[Cr+Al+Fe^{3+}]$.

rocks, these localities likely experienced comparable or more intense hydrothermal alteration (and associated element mobility) than the rocks at Hollofield Quarry; this might explain the extremely low total REEs but relatively high normalized La/Lu values for these rocks (Fig. 6). We therefore treat the incompatible bulk-rock trace element data with caution—particularly for those elements here considered to have been mobile—when interpreting the origin of the BMC (Origin of the Baltimore Mafic Complex section). Figure 6 highlights elements likely to be mobile in red, with these elements concentrated toward the left-hand side of the horizontal axis on both REE and trace element plots. The patterns and normalized abundances shown by the most compatible elements, which plot toward the right-hand side of these plots and are considered relatively immobile, are therefore considered the closest approximation of primary compositions.

Major element mobility is more difficult to constrain, but several general constraints can be made based on the data presented here. First, the high SiO_2 contents shown by most samples likely reflects high modal abundance of alteration phases. This is supported by the mineralogy of the samples with lowest SiO_2 contents (samples BMC19-H6 and BMC19-G2), which exhibit comparatively low modal abundances of alteration minerals (see Table 1 and Fig. 4). Second, the Soldiers Delight samples show a broad range in Ni and Cr contents, which can likely be attributed to variable alteration of Ni- and Cr-bearing phases in the low-Ni and low-Cr samples. In terms of Cr, this process is demonstrated by the alteration of spinel (see the Spinel Chemistry section below). The variation in Ni content is more ambiguous but could result from the removal of micrometer-scale pentlandite grains during hydrothermal alteration (e.g., Guice et al., 2019).

Spinel Chemistry: Distinguishing Primary and Secondary Compositions

The chemical compositions of spinel-group minerals in ultramafic rocks are extremely variable (cf. Kamenetsky et al., 2001; Barnes and Roeder, 2001) and may reflect diverse suites of processes, including

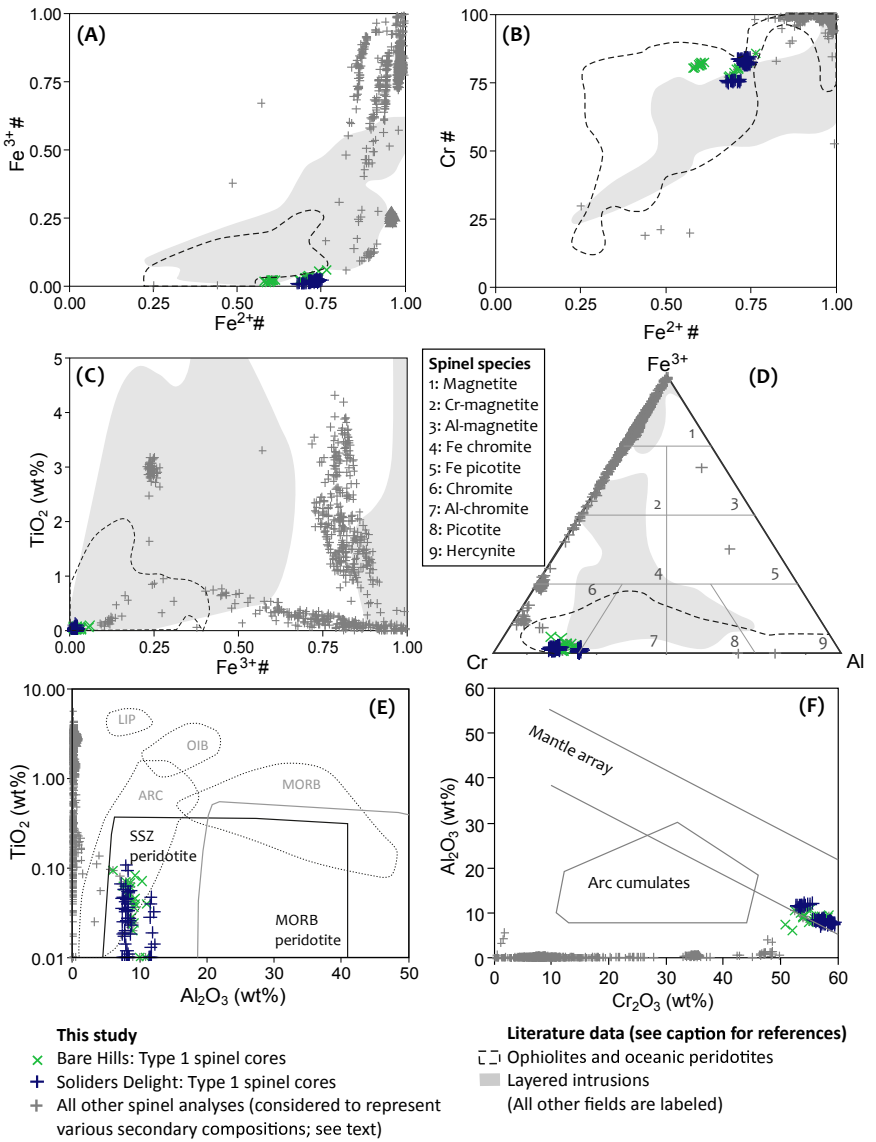

Figure 9. Composition of the type 1 spinel cores, which are considered to most closely resemble primary magmatic compositions. All other spinel analyses are included for reference. Cr# = molar Cr/[Cr/Al] x 100; Fe^{2+}# = molar $Fe^{2+}/[Mg+Fe^{2+}+Fe^{3+}]$; and Fe^{3+}# = molar $Fe^{3+}/[Cr+Al+Fe^{3+}]$. A–D are after Barnes and Roeder (2001); E, after Kamenetsky et al. (2001); F, after Kepezhinskas et al. (1995), Franz and Wirth (2000), and Kamenetsky et al. (2001). ARC—arc lavas; LIP—Large Igneous Province; MORB—mid-ocean ridge basalt; OIB—ocean island basalt; SSZ—suprasubduction zone.

primary crystallization, metamorphic growth, and chemical alteration associated with metamorphism and/or hydrothermal fluids (Lipin, 1984; Barnes and Roeder, 2001; Raymond et al., 2003; XuanThanh et al., 2011; Gargiulo et al., 2013; Ahmed and Surour, 2016). Based on the petrographic observations and chemical analyses presented in the Spinel Mineral Chemistry section above, spinel-group minerals in the BMC are interpreted to record both primary crystallization and secondary processes.

The homogeneous Al- and Cr-rich cores of the type 1 (distinctly zoned) grains show sharp chemical contrasts with the surrounding rims. On the bivariate plots presented in Figures 8 and 9, these analyses form tight clusters that are distinct from all other spinel groups and fall within the ophiolitic range established by Barnes and Roeder (2001), except for having slightly lower Fe^{3+}# values. These compositions, which are preserved only in the relatively coarse-grained spinel-group minerals found in the ultramafic rocks at Bare Hills and Soldiers Delight, are considered to represent primary compositions. This interpretation is consistent with the findings of Lipin (1984) and Gargiulo et al. (2013), who interpreted similar compositions as the product of magmatic crystallization.

All other compositions are considered to reflect one or more secondary processes; the thick rims shown by the type 1 spinel grains represent the clearest evidence that such compositions are secondary. Chemical analyses define a wide compositional array on bivariate and ternary plots between Cr-, Al-, Ti-, and Mn-rich cores to Fe-rich rims (Figs. 8–9). This same array is shown by the type 2 (cryptically zoned), type 3 (homogenous), and type 4 (partially rimmed) spinel grains from the studied localities, indicating that while any primary magmatic signatures in these grains are entirely obliterated, they record the same secondary process(es). This rim array—evolving along the ferritchromite-magnetite solid solution (Fig. 9D) toward the exterior of grains—is inconsistent with primary magmatic spinel fields (Fig. 9) and consistent with secondary spinel compositions documented at a variety of localities globally (e.g., Lipin, 1984; Barnes and Roeder, 2001; Raymond et al., 2003; XuanThanh et al., 2011; Gargiulo et al., 2013; Ahmed and Surour, 2016).

This broad array of secondary compositions can likely be attributed to one or more processes, which may include spinel growth during metamorphism, chemical alteration of existing (magmatic) spinel during metamorphism, and chemical alteration of existing (magmatic) spinel during serpentinization. Establishing the precise suite of metamorphic and hydrothermal processes responsible for the observed compositions is contingent upon a comprehensive understanding of the pressure-temperature conditions experienced by the BMC (and adjacent rocks), an understanding not afforded by the current body of literature. Most important, in the context of this paper, is the confident identification of type 1 spinel cores as resembling primary compositions that can be used to aid subsequent interpretations of the origin of the BMC (Fig. 9). Notably, all of these primary spinel compositions are from the Soldiers Delight and Bare Hills localities, with none from the Hollofield Ultramafite.

Origin of the Baltimore Mafic Complex

As outlined in the introduction to this paper, the BMC (and other ultramafic-mafic bodies in the central and southern Appalachians) have been previously considered to represent either ophiolite fragments (Crowley, 1976) or a dismembered stratiform intrusion (Shank and Marquez, 2014). In this section, we consider the origin of the Soldiers Delight Ultramafite before considering the Hollofield Ultramafite and Bare Hills ultramafic body (Fig. 1B). It should be noted that our interpretations should not be indiscriminately applied to the BMC in northern Maryland and southern Pennsylvania described by Shank and Marquez (2014). Although these rocks have historically been considered cogenetic, it is possible that they record multiple provenances, with further research required to establish the strength of previous correlations.

Soldiers Delight

As outlined in the Bulk-Rock Element Mobility section above, the concentrations of the elements that sit toward the right-hand side of chondrite-normalized REE and primitive mantle–normalized trace element plots (see Fig. 6) most closely resemble primary compositions and are utilized here for interpreting the origin of the BMC. The strongly depleted normalized bulk-rock trace element signatures observed for the Soldiers Delight Ultramafite (Fig. 6G) are highly suggestive of a mantle origin, with compositions overlapping strongly with the field for abyssal peridotites and ophiolitic mantle (see Figs. 5 and 6). In fact, the most compatible elements (e.g., Ho, Tm, Yb, and Lu) are even more depleted than these literature data for residual mantle rocks (Fig. 6G). This trace element signature is unique to mantle rocks that have experienced significant melt extraction, with incompatible elements lost to extracted melts (see the Introduction for details; e.g., Godard et al., 2000, 2008; Paulick et al., 2006). These data are therefore inconsistent with an intrusion-related interpretation for the origin of the Soldiers Delight Ultramafite (see Figs. 4–6 and 9).

A mantle origin for the Soldiers Delight Ultramafite is supported by other aspects of the bulk-rock and mineral chemical data. First, there is near-complete overlap between the bulk-rock compositions and the field for residual mantle rocks on both immobile trace element (see the Effects of Metamorphism and Hydrothermal Alteration section above for definition and discussion) bivariate plots (Fig. 5) and major element bivariate plots (Fig. 4). Second, type 1 spinel cores, which are considered to retain magmatic crystallization signatures (see the Spinel Chemistry: Distinguishing Primary and Secondary Compositions section above), show complete overlap with the field for ophiolites and oceanic peridotites (of Barnes and Roeder, 2001) on Fe^{2+}# versus Cr#, Fe^{3+}# versus TiO_2, and Cr-Fe^{3+}-Al plots (Figs. 9B–9D). For comparison, these data show minimal overlap with the large layered-intrusion field on the Fe^{2+}# versus Fe^{3+}#, Fe^{2+}# versus Cr#, Fe^{3+}# versus TiO_2, and Cr-Fe^{3+}-Al plots (Fig. 9). Third, these spinel analyses also fall within the suprasubduction zone (SSZ) peridotite field on the Al_2O_3 versus TiO_2 plot and within the mantle array on the Cr_2O_3 versus Al_2O_3 plot, and show the extremely low TiO_2 contents (<0.5 wt%) that are characteristic of podiform, rather than stratiform, chromitites (e.g., Kamenetsky et al., 2001). The analyses also show no overlap with the arc cumulates field on the Cr_2O_3 versus Al_2O_3 plot, underlining the inconsistency of these data with an arc-related intrusion interpretation (cf. Sinha et al., 1997; Shank and Marquez, 2014).

While the majority of data presented hint at a mantle origin for the Soldiers Delight Ultramafite, the position of magmatic spinel analyses on the Fe^{2+}# versus Fe^{3+}# plot (Fig. 9A) brings this interpretation into question, with the data showing only limited overlap with the ophiolites and abyssal peridotites field of Barnes and Roeder (2001). Despite this small inconsistency—likely attributable to alteration, which has demonstrably affected the Fe^{3+}# values of spinel (see Figs. 8–9)—we consider the Soldiers Delight Ultramafite to represent mantle peridotite (Fig. 10), with the broader BMC comprising various other ophiolitic fragments.

Hollofield Ultramafite

The presented data for the Hollofield Ultramafite show significant differences from those for Soldiers Delight (Figs. 4–6 and 8). First, the Hollofield Ultramafite is distinctly layered on millimeter, centimeter, and decimeter scales, as shown at the Hollofield Quarry (Figs. 2A–2B) and Forest Park Golf Course (Fig. 2C) localities (see Fig. 1 for locations). Second, these rocks are relatively evolved and distinct from the field for ophiolites and abyssal peridotites, exhibiting bulk-rock MgO contents of 17–33 wt% and TiO_2 contents >0.05 wt% (Fig. 4). Third, the geochemical data are consistent with rocks that crystallized *from* a melt, rather than being the residue after melt extraction. Primitive mantle–normalized trace element abundances are generally at or close to 1 (Figs. 6E–6F) and major element compositions are distinct from the field for mantle residue (see Fig. 4).

These data therefore suggest that the Hollofield Ultramafite crystallized from a melt, rather than representing residual mantle rocks. Given the probable mantle affiliation of the ultramafic rocks at Soldiers Delight (see the Soldiers Delight section above), the Hollofield Ultramafite could represent the

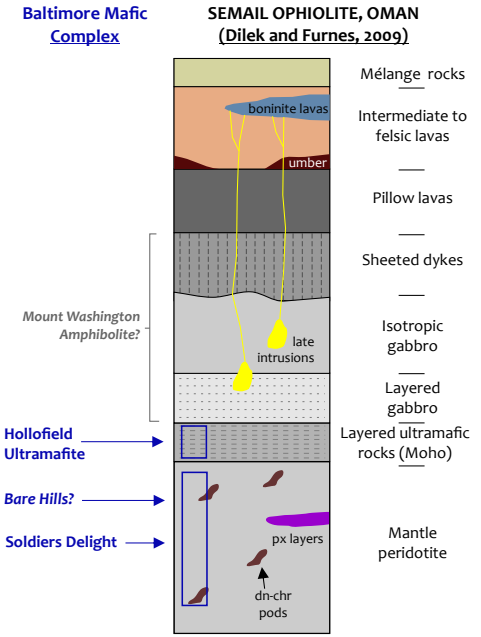

Figure 10. Schematic diagram detailing the stratigraphy of the Oman ophiolite (redrawn after Dilek and Furnes 2009), with the studied localities from the Baltimore Mafic Complex labeled within this ophiolite stratigraphy. Abbreviations: px—pyroxenite; dn-chr pods—dunite-chromitite pods.

ultramafic cumulates that form the Moho (Fig. 10; Dilek and Furnes, 2014). This interpretation is consistent with the spatial association with mafic rocks, which occur as volumetrically minor layers within the logged section at Hollofield Quarry (Fig. 2A) and predominate in the adjacent Mount Washington Amphibolite (Figs. 1B and 10).

Bare Hills

The Bare Hills ultramafic rocks share several bulk-rock geochemical and mineral chemical characteristics with the Soldiers Delight samples. First, the type 1 spinel cores plot within the ophiolite and oceanic peridotites field (of Barnes and Roeder 2001) on the Fe^{2+}# versus Cr#, Fe^{3+} versus TiO_2, and Cr-Fe^{3+}-Al plots, showing near-complete overlap with the Soldiers Delight analyses (Figs. 9B–9D). Second, these spinel data also plot within the SSZ peridotite and mantle array fields on the Al_2O_3 versus TiO_2 and Cr_2O_3 versus Al_2O_3 plots respectively (Figs. 9E–9F), and exhibit extremely low TiO_2 contents (cf. Kamenetsky et al. 2001). Third, the Bare Hills ultramafic rocks show near-complete overlap with the field for residual mantle rocks on most major element bivariate plots (Fig. 4).

Though these data suggest that the Bare Hills ultramafic body also represents mantle peridotite, this hypothesis is questioned by results shown in the normalized trace elements plot of Figure 6H, which indicates enrichment in trace elements relative to the field for residual mantle rocks. Such enrichment is observed not only for the more mobile elements (e.g., Rb, Ba, La) but also for the elements considered most immobile (see Fig. 6). While this geochemical signature could be explained by refertilization of mantle peridotite via interaction with mantle-derived melts, which has the effect of increasing trace element abundances and driving compositions back toward those for primitive mantle (Rollinson, 2007), we employ caution and consider the origin of this small occurrence (Fig. 1B) to remain ambiguous.

Magmatic Affinity of the BMC

To further elucidate the magmatic affinity of the BMC, the bulk-rock trace element compositions of the Soldiers Delight mantle rocks are compared to global data sets (see Fig. 11) compiled for three geodynamic settings (after Deschamps et al., 2013), namely: (1) abyssal serpentinites, which represent oceanic mantle peridotites formed at slow and ultraslow mid-ocean spreading ridges; (2) mantle wedge serpentinites, which can be broadly described as the mantle located between the upper part of subducting lithosphere and the overriding plate and can include forearc mantle; and (3) subducted serpentinites, which represent a more heterogenous and poorly defined group that includes mantle rocks from volatile-rich ridges, trenches, and the oceanic-continental transition zone.

On chondrite-normalized REE and primitive mantle–normalized trace element plots, the Soldiers Delight rocks are largely distinct from the field for abyssal serpentinites (Figs. 11A, 11D; Deschamps et al., 2013). While the Soldiers Delight samples show flat to mild positive slopes for the most compatible and immobile elements (Gd–Lu; Figs. 11A, 11D), abyssal serpentinites display steep positive slopes for these elements. Moreover, the Soldiers Delight samples show significant depletion in the most compatible elements (Yb and Lu) relative to abyssal serpentinites, suggesting the BMC does not represent oceanic lithosphere formed at a mid-ocean spreading ridge (i.e., the BMC is not a subduction-unrelated ophiolite; Dilek and Furnes, 2011). A spreading-ridge origin for the BMC is also contradicted by the composition of spinel in the Soldiers Delight mantle rocks. Spinel in abyssal peridotites generally shows Cr# <20 (Michael and Bonatti, 1985; Deschamps et al., 2013), whereas those analyzed from Soldiers Delight display Cr# of 75–86. Similarly, the Soldiers Delight mantle rocks show limited overlap with the subducted serpentinites field (Figs. 11C, 11F).

In contrast, the Soldiers Delight mantle rocks strongly correspond with the field for mantle wedge serpentinites (Figs. 11B, 11E), suggesting the BMC represents SSZ oceanic lithosphere (Dilek and Furnes, 2011). There is near-complete overlap with this field on both chondrite-normalized REE (Fig. 11B) and primitive mantle–normalized trace element plots (Fig. 11E). Despite this, some differences do exist from the mantle wedge serpentinites field. One sample shows extremely mild enrichment in most elements, and U is slightly enriched in most samples. A SSZ interpretation for the Soldiers Delight rocks is consistent with the primary compositions of spinel in these rocks (see the Spinel Chemistry: Distinguishing Primary and Secondary Compositions section above; Fig. 9), which plot within the SSZ peridotite field on the Al_2O_3 versus TiO_2 plot, display Cr# of between 75 and 85, and TiO_2 contents of ≤0.11 wt% (Fig. 9; Table 3). These data are comparable to those from spinel in subduction-related peridotites (including mantle wedge serpentinites), which generally show Cr# of >40 (Dick and Bullen, 1984; Parkinson and Arculus,

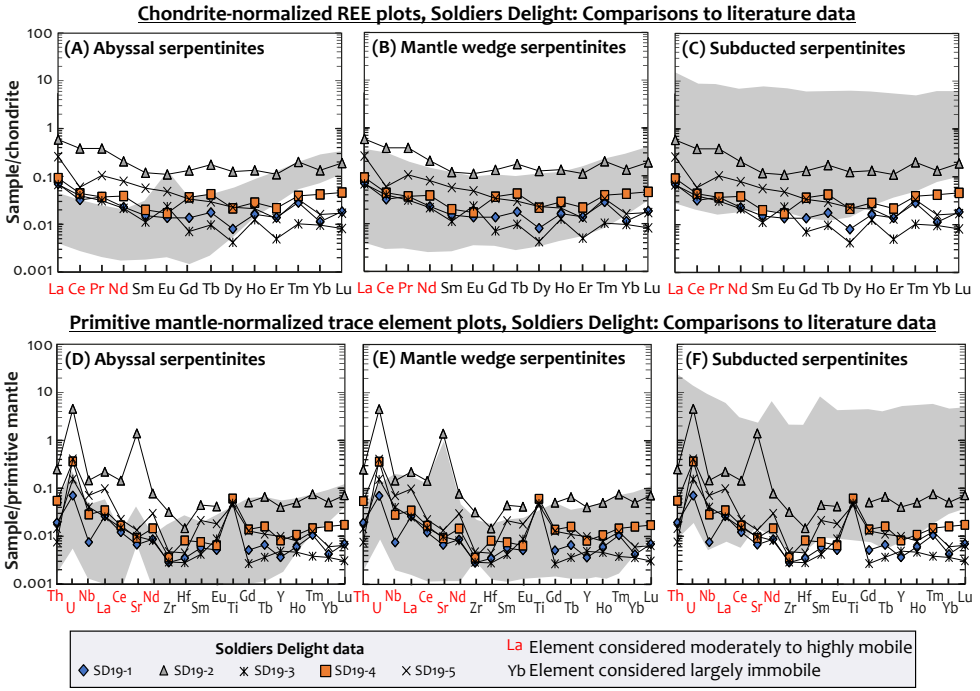

Figure 11. Chondrite-normalized rare earth element (REE) (A–C) and primitive mantle–normalized trace element (D–F) plots comparing the composition of mantle rocks from Soldiers Delight to global data sets for three geotectonic settings. Elements highlighted in red likely experienced mobility during metamorphism and alteration. See the Bulk-Rock Element Mobility section for full details. Fields are after Deschamps et al. (2013). Normalizing values are after McDonough and Sun (1995).

1999; Deschamps et al., 2013) and extremely low TiO_2 contents (Arai et al., 2011; Liu et al., 2016).

A subduction-related magmatic affinity for the BMC is also consistent with previous research focusing on the overlying mafic rocks (Hanan and Sinha, 1989; Sinha et al., 1997). The authors of that research interpreted the magmatic source as being associated with either a continental margin arc (Sinha et al., 1997) or back-arc basin–related magmatism (Hanan and Sinha, 1989). Further evaluation of these hypothesized settings—to more specifically elucidate ophiolite type—and our SSZ ophiolite interpretation should focus on utilizing modern geochemical methods to assess the geochemical affinity of the BMC's mafic lithologies. Specifically, further work needs to address the question of whether the BMC—like many other SSZ ophiolites globally (Whattam and Stern, 2011; Stern et al., 2012)—represents forearc crust recording evidence for subduction initiation, or else has a back-arc basin origin.

Potential Implications for the Evolution of the Appalachian Orogen

Ultramafic-mafic complexes occur along the entire length of the Appalachian orogen, from Alabama to Newfoundland. Recognition of lapetus-derived SSZ ophiolite fragments in the central Appalachian orogen raises interesting questions pertaining to the relationship to the northern Appalachian orogen, which also preserves SSZ ophiolites (e.g., Jenner et al., 1991; Olive et al., 1997; Bédard et al., 1998; Huot et al., 2002; Lissenberg et al., 2005; De Souza et al., 2008; Pagé et al., 2008, 2009; Pagé and Barnes, 2009). The possibility that broadly coeval ophiolites are preserved along thousands of kilometers of orogenic strike has potential implications for the initiation and evolution of tectonic convergence on a continental scale, within both the Appalachian orogen and orogenic belts globally. Key to addressing such questions will be further study of the Appalachian ultramafic-mafic complexes to better understand their timing and significance, in terms of both the magmatic and tectonic histories they record at specific localities and the along-strike timing of those events.

CONCLUSIONS

1. The primary finding of this study is that the Baltimore Mafic Complex in Maryland comprises several fragments of a suprasubduction zone (SSZ) ophiolite. The Soldiers Delight rocks likely represent mantle peridotites, with the Hollofield Ultramafite interpreted as the layered ultramafic portion that forms the Moho. The origin of the Bare Hills ultramafic body remains ambiguous.
2. Several ultramafic-mafic bodies in the central and southern Appalachians have previously been interpreted as ophiolite fragments, but this work presents, for the first time, chemical evidence for the presence of residual mantle rocks in this portion of the Appalachian orogen. Recognition of lapetus-derived SSZ ophiolite fragments in the central Appalachian orogen raises the interesting possibility that broadly coeval ophiolites are preserved along thousands of kilometers of orogenic strike.

ACKNOWLEDGMENTS

GLG would like to thank Tim Gooding and Rob Wardell for tireless assistance in a pantheon of areas, including thin-section production, thin-section photography, preparation of samples

for bulk-rock geochemical analysis, and preparation of samples for mineral analysis. We would like to thank LeeAnn Srogi and Yildirim Dilek for constructive, detailed reviews that have greatly improved the quality of this manuscript and its scope. We would also like to thank managing editor Gina Harlow, science editor Andrea Hampel, and Associate Editor Alan Whittington for efficient handling of the manuscript.

REFERENCES CITED

Adams, M.G., Stewart, K.G., Trupe, C.H., and Willard, R.A., 1994, Tectonic significance of high-pressure metamorphic rocks and dextral strike-slip faulting in the southern Appalachians: Atlantic Geology, v. 30, p. 162.

Ahmed, A.H., and Surour, A.A., 2016, Fluid-related modifications of Cr-spinel and olivine from ophiolitic peridotites by contact metamorphism of granitic intrusions in the Ablah area, Saudi Arabia: Journal of Asian Earth Sciences, v. 122, p. 58–79, https://doi.org/10.1016/j.jseaes.2016.03.010.

Aleinikoff, J.N., Horton, J.W., Jr., Drake, A.A., Jr., and Fanning, C.M., 2002, SHRIMP and conventional U-Pb ages of Ordovician granites and tonalites in the central Appalachian Piedmont: Implications for Paleozoic tectonic events: American Journal of Science, v. 302, p. 50–75, https://doi.org/10.2475/ajs.302.1.50.

Arai, S., Okamura, H., Kadoshima, K., Tanaka, C., Suzuki, K., and Ishimaru, S., 2011, Chemical characteristics of chromian spinel in plutonic rocks: Implications for deep magma processes and discrimination of tectonic setting: Island Arc, v. 20, p. 125–137, https://doi.org/10.1111/j.1440-1738.2010.00747.x.

Barnes, S.J., and Roeder, P.L., 2001, The range of spinel compositions in terrestrial mafic and ultramafic rocks: Journal of Petrology, v. 42, p. 2279–2302, https://doi.org/10.1093/petrology/42.12.2279.

Bascom, F., 1902, The Geology of the Crystalline Rocks of Cecil County: Baltimore, Johns Hopkins Press, 147 p.

Bédard, J.H., Lauzière, K., Tremblay, A., and Sangster, A., 1998, Evidence for forearc seafloor-spreading from the Betts Cove ophiolite, Newfoundland: Oceanic crust of boninitic affinity: Tectonophysics, v. 284, p. 233–245, https://doi.org/10.1016/S0040-1951(97)00182-0.

Bosbyshell, H., Srogi, L., and Blackmer, G.C., 2016, Monazite age constraints on the tectono-thermal evolution of the central Appalachian Piedmont: American Mineralogist, v. 101, p. 1820–1838, https://doi.org/10.2138/am-2016-5482.

Burgess, J.L., Lev, S., Swan, C.M., and Szlavecz, K., 2009, Geologic and edaphic controls on a serpentine forest community: Northeastern Naturalist, v. 16, p. 366–384, https://doi.org/10.1656/045.016.0527.

Cawthorn, R.G., Barnes, S.J., Ballhaus, C., and Malitch, K.N., 2005, Platinum group element, chromium, and vanadium deposits in mafic and ultramafic rocks, *in* Hedenquist, J.W., Thompson, J.F.H., Goldfarb, R.J., and Richards, J.P., eds., Economic Geology: One Hundredth Anniversary Volume: Littleton, Colorado, Society of Economic Geologists, Inc., p. 215–249, https://doi.org/10.5382/AV100.09.

Church, W.R., and Stevens, R.K., 1971, Early Paleozoic ophiolite complexes of the Newfoundland Appalachians as mantle-oceanic crust sequences: Journal of Geophysical Research, v. 76, p. 1460–1466, https://doi.org/10.1029/JB076i005p01460.

Cleaves, E.T., Crowley, W.P., and Kuff, K.R., 1974, Towson quadrangle: Geologic and environmental atlas: Maryland Geologic Survey Quadrangle Atlas 2, 5 sheets, scale 1:24,000.

Coish, R.A., and Gardner, P., 2004, Suprasubduction-zone peridotite in the northern USA Appalachians: Evidence from mineral composition: Mineralogical Magazine, v. 68, p. 699–708, https://doi.org/10.1180/0026461046840214.

Crowley, W.P., 1976, The geology of the crystalline rocks near Baltimore and its bearing on the evolution of the eastern Maryland Piedmont: Maryland Geologic Survey Report of Investigations 27, 2 sheets, with 40 p. text.

Crowley, W.P., and Reinhardt, J., 1979, Geologic map of the Baltimore West quadrangle: Baltimore, Maryland Geological Survey, scale 1:24,000.

Crowley, W.P., Reinhart, J., and Cleaves, E.T., 1975, Geologic map of the Cockeysville quadrangle, Maryland: Baltimore, Maryland Geological Survey, scale 1:24,000.

Deschamps, F., Godard, M., Guillot, S., and Hattori, K., 2013, Geochemistry of subduction zone serpentinites: A review: Lithos, v. 178, p. 96–127, https://doi.org/10.1016/j.lithos.2013.05.019.

De Souza, S., Tremblay, A., Daoust, C., and Gauthier, M., 2008, Stratigraphy and geochemistry of the Lac-Brompton ophiolite, Canada: Evidence for extensive forearc magmatism and mantle exhumation in the Southern Quebec Ophiolite Belt: Canadian Journal of Earth Sciences, v. 45, p. 999–1014, https://doi.org/10.1139/E08-044.

Dick, H.J.B., and Bullen, T., 1984, Chromian spinel as a petrogenetic indicator in abyssal and alpine-type peridotites and spatially associated lavas: Contributions to Mineralogy and Petrology, v. 86, p. 54–76, https://doi.org/10.1007/BF00373711.

Dilek, Y., and Furnes, H., 2009, Structure and geochemistry of Tethyan ophiolites and their petrogenesis in subduction rollback systems: Lithos, v. 113, p. 1–20, https://doi.org/10.1016/j.lithos.2009.04.022.

Dilek, Y., and Furnes, H., 2011, Ophiolite genesis and global tectonics: Geochemical and tectonic fingerprinting of ancient oceanic lithosphere: Geological Society of America Bulletin, v. 123, p. 387–411, https://doi.org/10.1130/B30446.1.

Dilek, Y., and Furnes, H., 2014, Ophiolites and their origins: Elements, v. 10, p. 93–100, https://doi.org/10.2113/gselements.10.2.93.

Drake, A.A., Jr., 1998, Geologic map of the Piedmont in the Savage and Relay quadrangles, Howard, Baltimore, and Anne Arundel Counties, Maryland: U.S. Geological Survey Open-File Report 98-757, 1 sheet, scale 1:24,000, with 30 p. text, https://doi.org/10.3133/ofr98757.

Drake, A.A., Jr., and Morgan, B.A., 1981, The Piney Branch Complex—A metamorphosed fragment of the central Appalachian ophiolite in northern Virginia: American Journal of Science, v. 281, p. 484–508, https://doi.org/10.2475/ajs.281.4.484.

Droop, G.T.R., 1987, A general equation for estimating Fe^{3+} concentrations in ferromagnesian silicates and oxides from microprobe analyses, using stoichiometric criteria: Mineralogical Magazine, v. 51, p. 431–435, https://doi.org/10.1180/minmag.1987.051.361.10.

Escayola, M., Garuti, G., Zaccarini, F., Proenza, J.A., Bédard, J.H., and Van Staal, C., 2011, Chromitite and platinum-group-element mineralization at Middle Arm Brook, central Advocate ophiolite complex, Baie Verte Peninsula, Newfoundland, Canada: Canadian Mineralogist, v. 49, p. 1523–1547, https://doi.org/10.3749/canmin.49.6.1523.

Faill, R.T., 1997, A geologic history of the north-central Appalachians: Part 1, Orogenesis from the Mesoproterozoic through the Taconic Orogeny: American Journal of Science, v. 297, p. 551–619, https://doi.org/10.2475/ajs.297.6.551.

Franz, L., and Wirth, R., 2000, Spinel inclusions in olivine of peridotite xenoliths from TUBAF seamount (Bismarck Archipelago/Papua New Guinea): Evidence for the thermal and tectonic evolution of the oceanic lithosphere: Contributions to Mineralogy and Petrology, v. 140, p. 283–295, https://doi.org/10.1007/s004100000188.

Gargiulo, M.F., Bjerg, E.A., and Mogessie, A., 2013, Spinel group minerals in metamorphosed ultramafic rocks from Río de Las Tunas belt, Central Andes, Argentina: Geologica Acta, v. 11, p. 133–148, https://doi.org/10.1344/105.000001836.

Gates, A.E., 1992, Domainal failure of serpentinite in shear zones, State-Line mafic complex, Pennsylvania, U.S.A.: Journal of Structural Geology, v. 14, p. 19–28, https://doi.org/10.1016/0191-8141(92)90141-I.

Gates, A.E., Muller, P.D., and Krol, M.A., 1999, Alleghanian transpressional orogenic float in the Baltimore terrane, central Appalachian Piedmont, *in* Valentino, D.W., and Gates, A.E., eds., The Mid-Atlantic Piedmont: Tectonic Missing Link of the Appalachians: Geological Society of America Special Paper 330, p. 127–139, https://doi.org/10.1130/0-8137-2330-2.127.

Godard, M., Jousselin, D., and Bodinier, J.-L., 2000, Relationships between geochemistry and structure beneath a palaeo-spreading centre: A study of the mantle section in the Oman ophiolite: Earth and Planetary Science Letters, v. 180, p. 133–148, https://doi.org/10.1016/S0012-821X(00)00149-7.

Godard, M., Lagabrielle, Y., Alard, O., and Harvey, J., 2008, Geochemistry of the highly depleted peridotites drilled at ODP Sites 1272 and 1274 (Fifteen-Twenty Fracture Zone, Mid-Atlantic Ridge): Implications for mantle dynamics beneath a slow spreading ridge: Earth and Planetary Science Letters, v. 267, p. 410–425, https://doi.org/10.1016/j.epsl.2007.11.058.

Guice, G.L., 2019, Origin and geodynamic significance of ultramafic-mafic complexes in the North Atlantic and Kaapvaal Cratons [Ph.D. thesis]: Cardiff, UK, Cardiff University, 289 p., http://orca.cf.ac.uk/123339/.

Guice, G.L., McDonald, I., Hughes, H.S.R., Schlatter, D.M., Goodenough, K.M., MacDonald, J.M., and Faithfull, J.W., 2018, Assessing the validity of negative high field strength-element anomalies as a proxy for Archaean subduction: Evidence from the Ben Strome Complex, NW Scotland: Geosciences, v. 8, 338, https://doi.org/10.3390/geosciences8090338.

Guice, G.L., McDonald, I., Hughes, H.S.R., and Anhaeusser, C.R., 2019, An evaluation of element mobility in the Modderfontein ultramafic complex, Johannesburg: Origin as an Archaean ophiolite fragment or greenstone belt remnant?: Lithos, v. 332–333, p. 99–119, https://doi.org/10.1016/j.lithos.2019.02.013.

Hanan, B.B., and Sinha, A.K., 1989, Petrology and tectonic affinity of the Baltimore mafic complex, Maryland, *in* Mittwede, S.K., and Stoddard, E.F., eds., Ultramafic Rocks of the Appalachian Piedmont: Geological Society of America Special Paper 231, p. 1–18, https://doi.org/10.1130/SPE231-p1.

Hatcher, R.D., Jr., 1987, Tectonics of the southern and central Appalachian internides (USA): Annual Review of Earth and

Planetary Sciences, v. 15, p. 337–362, https://doi.org/10.1146/annurev.earth.15.1.337.

Hatcher, R.D., Jr., 2004, North America: Southern and central Appalachians, *in* Selley, R.C., Cocks, L.R.M., and Plimer, I.R., eds., Encyclopedia of Geology: Academic Press, v. 1, p. 72–81, https://doi.org/10.1016/B0-12-369396-9/00408-1.

Hatcher, R.D., Jr., 2010, The Appalachian orogen: A brief summary, *in* Tollo, R.P., Bartholomew, M.J., Hibbard, J.P., and Karabinos, P.M., eds., From Rodinia to Pangea: The Lithotectonic Record of the Appalachian Region: Geological Society of America Memoir 206, p. 1–19, https://doi.org/10.1130/2010.1206(01).

Hibbard, J.P., 2006, Lithotectonic map of the Appalachian orogen, Canada–United States of America: Geological Survey of Canada Map 02096A, 2 sheets, scale 1:1,500,000.

Hibbard, J.P., Shell, G.S., Bradley, P.J., Samson, S.D., and Wortman, G.L., 1998, The Hyco shear zone in North Carolina and southern Virginia: Implications for the Piedmont Zone–Carolina Zone boundary in the Southern Appalachians: American Journal of Science, v. 298, p. 85–107, https://doi.org/10.2475/ajs.298.2.85.

Hibbard, J.P., van Staal, C.R., and Miller, B.V., 2007a, Links among Carolinia, Avalonia, and Ganderia in the Appalachian peri-Gondwanan realm, *in* Sears, J.W., Harms, T.A., and Evenchick, C.A., eds., Whence the Mountains? Inquiries into the Evolution of Orogenic Systems: A Volume in Honor of Raymond A. Price: Geological Society of America Special Paper 433, p. 291–311, https://doi.org/10.1130/2007.2433(14).

Hibbard, J.P., van Staal, C.R., and Rankin, D.W., 2007b, A comparative analysis of pre-Silurian crustal building blocks of the northern and the southern Appalachian orogen: American Journal of Science, v. 307, p. 23–45, https://doi.org/10.2475/01.2007.02.

Higgins, M.D., Sinha, A.K., Zartman, R.E., and Kirk, W.S., 1977, U-Pb zircon dates from the central Appalachian Piedmont: A possible case of inherited radiogenic lead: Geological Society of America Bulletin, v. 88, p. 125–132, https://doi.org/10.1130/0016-7606(1977)88<125:UZDFTC>2.0.CO;2.

Hopson, C.A., 1964, The Crystalline Rocks of Howard and Montgomery Counties: Baltimore, Maryland Geologic Survey, 371 p.

Horton, J.W., Drake, A.A., and Rankin, D.W., 1989, Tectonostratigraphic terranes and their Paleozoic boundaries in the central and southern Appalachians, *in* Dallmeyer, R.D., eds., Terranes in the Circum-Atlantic Paleozoic Orogens: Geological Society of America Special Paper 230, p. 213–246, https://doi.org/10.1130/SPE230-p213.

Horton, J.W., Jr., Aleinikoff, J.N., Drake, A.A., Jr., and Fanning, C.M., 2010, Ordovician volcanic-arc terrane in the Central Appalachian Piedmont of Maryland and Virginia: SHRIMP U-Pb geochronology, field relations, and tectonic significance, *in* Tollo, R.P., Bartholomew, M.J., Hibbard, J.P., and Karabinos, P.M., eds., From Rodinia to Pangea: The Lithotectonic Record of the Appalachian Region: Geological Society of America Memoir 206, p. 621–660, https://doi.org/10.1130/2010.1206(25).

Huot, F., Hébert, R., and Turcotte, B., 2002, A multistage magmatic history for the genesis of the Orford ophiolite (Quebec, Canada): A study of the Mont Chagnon massif: Canadian Journal of Earth Sciences, v. 39, p. 1201–1217, https://doi.org/10.1139/e02-030.

Jenner, G.A., Dunning, G.R., Malpas, J., Brown, M., and Brace, T., 1991, Bay of Islands and Little Port complexes, revisited: Age, geochemical and isotopic evidence confirm suprasubduction-zone origin: Canadian Journal of Earth Sciences, v. 28, p. 1635–1652, https://doi.org/10.1139/e91-146.

Johnsson, J., 2017, Maryland's Choate chromite mine, 1830–1920: The Mining History Journal, v. 24, p. 53–73, https://www.mininghistoryassociation.org/Journal/MHJ-v24-2017-Johnsson.pdf (accessed January 2020).

Kamenetsky, V.S., Crawford, A.J., and Meffre, S., 2001, Factors controlling chemistry of magmatic spinel: An empirical study of associated olivine, Cr-spinel and melt inclusions from primitive rocks: Journal of Petrology, v. 42, p. 655–671, https://doi.org/10.1093/petrology/42.4.655.

Kepezhinskas, P.K., Defant, M.J., and Drummond, M.S., 1995, Na metasomatism in the island-arc mantle by slab melt–peridotite interaction: Evidence from mantle xenoliths in the north Kamchatka arc: Journal of Petrology, v. 36, p. 1505–1527, https://doi.org/10.1093/oxfordjournals.petrology.a037263.

Kerrigan, R.J., Mengason, M.J., and Simboli, L.N., 2017, Petrology and geochemistry of the Bells Mill Road ultramafic body, Philadelphia PA, *in* Bosbyshell, H., ed., The Piedmont: Old Rocks, New Understandings: 2017 Conference Proceedings for the 34th Annual Meeting of the Geological Association of New Jersey: Trenton, Geological Association of New Jersey, p. 16–29.

Kim, J., Coish, R., Evans, M., and Dick, G., 2003, Supra-subduction zone extensional magmatism in Vermont and adjacent Quebec: Implications for early Paleozoic Appalachian tectonics: Geological Society of America Bulletin, v. 115, p. 1552–1569, https://doi.org/10.1130/B25343.1.

Kurth-Velz, M., Sassen, A., and Galer, S.J.G., 2004, Geochemical and isotopic heterogeneities along an island arc–spreading ridge intersection: Evidence from the Lewis Hills, Bay of Islands Ophiolite, Newfoundland: Journal of Petrology, v. 45, p. 635–668, https://doi.org/10.1093/petrology/egg096.

Lahaye, Y., Arndt, N., Byerly, G., Chauvel, C., Fourcade, S., and Gruau, G., 1995, The influence of alteration on the trace-element and Nd isotopic compositions of komatiites: Chemical Geology, v. 126, p. 43–64, https://doi.org/10.1016/0009-2541(95)00102-1.

Lavoie, D., Burden, E., and Lebel, D., 2003, Stratigraphic framework for the Cambrian–Ordovician rift and passive margin successions from southern Quebec to western Newfoundland: Canadian Journal of Earth Sciences, v. 40, p. 177–205, https://doi.org/10.1139/e02-078.

Leonard, A.G., 1901, The basic rocks of northeastern Maryland and their relation to the granite [Ph.D. thesis]: Baltimore, Johns Hopkins University, 177 p.

Lipin, B.R., 1984, Chromite from the Blue Ridge province of North Carolina: American Journal of Science, v. 284, p. 507–529, https://doi.org/10.2475/ajs.284.4-5.507.

Lissenberg, C.J., van Staal, C.R., Bédard, J.H., and Zagorevski, A., 2005, Geochemical constraints on the origin of the Annieopsquotch ophiolite belt, Newfoundland Appalachians: Geological Society of America Bulletin, v. 117, p. 1413–1426, https://doi.org/10.1130/B25731.1.

Liu, C.-Z., Zhang, C., Xu, Y., Wang, J.-G., Chen, Y., Guo, S., Wu, F.-Y., and Sein, K., 2016, Petrology and geochemistry of mantle peridotites from the Kalaymyo and Myitkyina ophiolites (Myanmar): Implications for tectonic settings: Lithos, v. 264, p. 495–508, https://doi.org/10.1016/j.lithos.2016.09.013.

McDonough, W.F., and Sun, S.-s., 1995, The composition of the Earth: Chemical Geology, v. 120, p. 223–253, https://doi.org/10.1016/0009-2541(94)00140-4.

McElhaney, M.S., and McSween, H.Y., Jr., 1983, Petrology of the Chunky Gal Mountain mafic-ultramafic complex, North Carolina: Geological Society of America Bulletin, v. 94, p. 855–874, https://doi.org/10.1130/0016-7606(1983)94<855:POTCGM>2.0.CO;2.

Michael, P.J., and Bonatti, E., 1985, Peridotite composition from the North Atlantic: Regional and tectonic variations and implications for partial melting: Earth and Planetary Science Letters, v. 73, p. 91–104, https://doi.org/10.1016/0012-821X(85)90037-8.

Misra, K.C., and Conte, J.A., 1991, Amphibolites of the Ashe and Alligator Back Formations, North Carolina: Samples of late Proterozoic–early Paleozoic oceanic crust: Geological Society of America Bulletin, v. 103, p. 737–750, https://doi.org/10.1130/0016-7606(1991)103<0737:AOTAAA>2.3.CO;2.

Misra, K.C., and Keller, F.B., 1978, Ultramafic bodies in the Southern Appalachians: A review: American Journal of Science, v. 278, p. 389–418, https://doi.org/10.2475/ajs.278.4.389.

Mittwede, S.K., 1989, The Hammett Grove Meta-igneous Suite: A possible ophiolite in the northwestern South Carolina Piedmont, *in* Mittwede, S.K., and Stoddard, E.F., eds., Ultramafic Rocks of the Appalachian Piedmont: Geological Society of America Special Paper 231, p. 45–62, https://doi.org/10.1130/SPE231-p45.

Monteiro, L.V.S., Xavier, R.P., Hitzman, M.W., Juliani, C., de Souza Filho, C.R., and Carvalho, E. de R., 2008, Mineral chemistry of ore and hydrothermal alteration at the Sossego iron oxide-copper-gold deposit, Carajás Mineral Province, Brazil: Ore Geology Reviews, v. 34, p. 317–336, https://doi.org/10.1016/j.oregeorev.2008.01.003.

Murphy, J.B., Keppie, J.D., Nance, R.D., and Dostal, J., 2010, Comparative evolution of the Iapetus and Rheic Oceans: A North America perspective: Gondwana Research, v. 17, p. 482–499, https://doi.org/10.1016/j.gr.2009.08.009.

Olive, V., Hébert, R., and Loubet, M., 1997, Isotopic and trace element constraints on the genesis of a boninitic sequence in the Thetford Mines ophiolitic complex, Quebec, Canada: Canadian Journal of Earth Sciences, v. 34, p. 1258–1271, https://doi.org/10.1139/e17-100.

Pagé, P., and Barnes, S.-J., 2009, Using trace elements in chromites to constrain the origin of podiform chromitites in the Thetford Mines Ophiolite, Québec, Canada: Economic Geology and the Bulletin of the Society of Economic Geologists, v. 104, p. 997–1018, https://doi.org/10.2113/econgeo.104.7.997.

Pagé, P., Bédard, J.H., Schroetter, J.-M., and Tremblay, A., 2008, Mantle petrology and mineralogy of the Thetford Mines Ophiolite Complex: Lithos, v. 100, p. 255–292, https://doi.org/10.1016/j.lithos.2007.06.017.

Pagé, P., Bédard, J.H., and Tremblay, A., 2009, Geochemical variations in a depleted fore-arc mantle: The Ordovician Thetford Mines Ophiolite: Lithos, v. 113, p. 21–47, https://doi.org/10.1016/j.lithos.2009.03.030.

Parkinson, I.J., and Arculus, R.J., 1999, The redox state of subduction zones: Insights from arc-peridotites: Chemical Geology, v. 160, p. 409–423, https://doi.org/10.1016/S0009-2541(99)00110-2.

Paulick, H., Bach, W., Godard, M., De Hoog, J.C.M., Suhr, G., and Harvey, J., 2006, Geochemistry of abyssal peridotites (Mid-Atlantic Ridge, 15° 20′N, ODP Leg 209): Implications for fluid/rock interaction in slow spreading environments: Chemical Geology, v. 234, p. 179–210, https://doi.org/10.1016/j.chemgeo.2006.04.011.

Peterson, V., and Ryan, J.G., 2009, Petrogenesis and structure of the Buck Creek mafic-ultramafic suite, Southern Appalachians: Constraints on ophiolite evolution and emplacement in collisional orogens: Geological Society of America Bulletin, v. 121, p. 615–629, https://doi.org/10.1130/B26302.1.

Powell, W., Zhang, M., O'Reilly, S.Y., and Tiepolo, M., 2004, Mantle amphibole trace-element and isotopic signatures trace multiple metasomatic episodes in lithospheric mantle, western Victoria, Australia: Lithos, v. 75, p. 141–171, https://doi.org/10.1016/j.lithos.2003.12.017.

Rankin, D.W., 1975, The continental margin of eastern North America in the southern Appalachians: The opening and closing of the proto–Atlantic Ocean: American Journal of Science, v. 275-A, p. 298–336.

Raymond, L.A., Swanson, S.E., Love, A.B., and Allan, J.F., 2003, Cr-spinel compositions, metadunite petrology, and the petrotectonic history of Blue Ridge ophiolites, Southern Appalachian Orogen, USA, *in* Dilek, Y., and Robinson, P.T., eds., Ophiolites in Earth History: Geological Society of London Special Publication 218, p. 253–278, https://doi.org/10.1144/GSL.SP.2003.218.01.14.

Raymond, L.A., Merschat, A., and Vance, R.K., 2016, Metaultramafic schists and dismembered ophiolites of the Ashe Metamorphic Suite of northwestern North Carolina, USA: International Geology Review, v. 58, p. 874–912, https://doi.org/10.1080/00206814.2015.1129515.

Reinhardt, J., and Crowley, W.P., 1979, Geologic map of the Baltimore East quadrangle: Baltimore, Maryland Geologic Survey, 1 sheet, scale 1:24,000.

Rodgers, J., 1968, The eastern edge of the North American continent during the Cambrian and Early Ordovician, *in* Zen, E.-a., White, W.S., Hadley, J.B., and Thompson, J.B., Jr., eds., Studies of Appalachian Geology: Northern and Maritime: New York, Wiley-Interscience, p. 141–149.

Rodgers, J., 1970, Tectonics of the Appalachians: New York, Wiley-Interscience, 271 p.

Rollinson, H., 2007, Recognising early Archaean mantle: A reappraisal: Contributions to Mineralogy and Petrology, v. 154, p. 241–252, https://doi.org/10.1007/s00410-007-0191-y.

Shank, S., and Marquez, L., 2014, Geology of the Baltimore mafic complex in the Pennsylvania-Maryland state line area, *in* Cressler, W.L., Bosbyshell, H., and Srogi, L.A., eds., Field Trip Guide: Northeastern Section of the Geological Society of America, March 2014, Lancaster, Pennsylvania, p. 35–52.

Shaw, H.F., and Wasserburg, G.J., 1984, Isotopic constraints on the origin of Appalachian mafic complexes: American Journal of Science, v. 284, p. 319–349, https://doi.org/10.2475/ajs.284.4-5.319.

Sinha, A.K., Hanan, B.B., and Wayne, D.M., 1997, Igneous and metamorphic U-Pb zircon ages from the Baltimore mafic complex, Maryland Piedmont, *in* Sinha, A.K., Whalen, J.B., and Hogan, J.P., eds., The Nature of Magmatism in the Appalachian Orogen: Geological Society of America Memoir 191, p. 275–285, https://doi.org/10.1130/0-8137-1191-6.275.

Sinha, A.K., Thomas, W.A., Hatcher, R.D., and Harrison, T.M., 2012, Geodynamic evolution of the central Appalachian orogen: Geochronology and compositional diversity of magmatism from Ordovician through Devonian: American Journal of Science, v. 312, p. 907–966, https://doi.org/10.2475/08.2012.03.

Southwick, D.L., 1969, Crystalline rocks of Harford County *in* The Geology of Harford County, Maryland: Maryland Geological Survey County Report 16, p. 1–76.

Stern, R.J., Reagan, M., Ishizuka, O., Ohara, Y., and Whattam, S., 2012, To understand subduction initiation, study forearc crust: To understand forearc crust, study ophiolites: Lithosphere, v. 4, p. 469–483, https://doi.org/10.1130/L183.1.

Stow, S.H., Neilson, M.J., and Neathery, T.L., 1984, Petrography, geochemistry, and tectonic significance of the amphibolites of the Alabama Piedmont: American Journal of Science, v. 284, p. 414–436, https://doi.org/10.2475/ajs.284.4-5.414.

Tenthorey, E.A., Ryan, J.G., and Snow, E.A., 1996, Petrogenesis of sapphirine-bearing metatroctolites from the Buck Creek ultramafic body, southern Appalachians: Journal of Metamorphic Geology, v. 14, p. 103–114, https://doi.org/10.1046/j.1525-1314.1996.05793.x.

Thomas, W.A., 1977, Evolution of Appalachian-Ouachita salients and recesses from reentrants and promontories in the continental margin: American Journal of Science, v. 277, p. 1233–1278, https://doi.org/10.2475/ajs.277.10.1233.

Whattam, S.A., and Stern, R.J., 2011, The "subduction initiation rule": A key for linking ophiolites, intra-oceanic forearcs, and subduction initiation: Contributions to Mineralogy and Petrology, v. 162, p. 1031–1045, https://doi.org/10.1007/s00410-011-0638-z.

Williams, H., 1977, Ophiolitic mélange and its significance in the Fleur de Lys Supergroup, northern Appalachians: Canadian Journal of Earth Sciences, v. 14, p. 987–1003, https://doi.org/10.1139/e77-091.

Williams, H., and Hatcher, R.D., Jr., 1982, Suspect terranes and accretionary history of the Appalachian orogen: Geology, v. 10, p. 530–536, https://doi.org/10.1130/0091-7613(1982)10<530:STAAHO>2.0.CO;2.

Wood, B.J., 1990, An experimental test of the spinel peridotite oxygen barometer: Journal of Geophysical Research, v. 95, p. 15,845–15,851, https://doi.org/10.1029/JB095iB10p15845.

XuanThanh, N., Tu, M.T., Itaya, T., and Kwon, S., 2011, Chromian-spinel compositions from the Bo Xinh ultramafics, Northern Vietnam: Implications on tectonic evolution of the Indochina block: Journal of Asian Earth Sciences, v. 42, p. 258–267, https://doi.org/10.1016/j.jseaes.2011.02.004.

Yaxley, G.M., Crawford, A.J., and Green, D.H., 1991, Evidence for carbonatite metasomatism in spinel peridotite xenoliths from western Victoria, Australia: Earth and Planetary Science Letters, v. 107, p. 305–317, https://doi.org/10.1016/0012-821X(91)90078-V.